Ocean-scale connectivity and life cycle reconstruction in a deep-sea fish

Craig Longmore, Clive N. Trueman, Francis Neat, Per Erik Jorde, Halvor Knutsen, Sergio Stefanni, Diana Catarino, James A. Milton, Stefano Mariani

This is the author's version of an article published in the journal:

Canadian Journal of Fisheries and Aquatic Sciences, 2014, 71(9), 1312-1323

doi: 10.1139/cjfas-2013-0343

Canadian Journal of
Fisheries and Aquatic Sciences
Journal canadienne des
sciences halieutiques et
aquatiques

Oceanic scale connectivity and life cycle reconstruction in a deep-sea fish

Journal:	*Canadian Journal of Fisheries and Aquatic Sciences*
Manuscript ID:	cjfas-2013-0343.R2
Manuscript Type:	Article
Date Submitted by the Author:	06-Jan-2014
Complete List of Authors:	Longmore, Craig; University of Southampton, National Oceanography Centre, Ocean & Earth Sciences Trueman, Clive; University of Southampton, National Oceanography Centre Neat, Francis; Marine Scotland—Science, The Marine Laboratory, Jorde, Per Erik; Centre for Ecological and Evolutionary Synthesis (CEES), University of Oslo, Department of Biosciences, University of Oslo; Institute of Marine Research, Knutsen, Halvor; Institute of Marine Research; Centre for Ecological and Evolutionary Synthesis (CEES), University of Oslo, Department of Biosciences, University of Oslo; Institute of Marine Research, ; University of Agder, Department of Natural Sciences Stefanni, Sergio; LARSyS – Associated Laboratory & Centre of IMAR of the University of the Azores, Department of Oceanography and Fisheries Catarino, Diana; LARSyS – Associated Laboratory & Centre of IMAR of the University of the Azores, Department of Oceanography and Fisheries Milton, James; University of Southampton, National Oceanography Centre Mariani, Stefano; The University of Salford, School of Environment & Life Sciences
Keyword:	Deep-sea ecology, POPULATION STRUCTURE < General, Otolith microchemistry, GENETICS < General, Stable isotope analysis

Oceanic scale connectivity and life cycle reconstruction in a deep-sea fish

Longmore C.*[a], Trueman C. N.[a], Neat F.[b], Jorde P.E.[c, d], Knutsen H.[c, d,e], Stefanni S.[f], Catarino D.[f], Milton J. A.[a] & Mariani S.[g]

a: Ocean and Earth Science, University of Southampton Waterfront Campus, European Way, Southampton SO14 3ZH, UK

b: Marine Scotland—Science, The Marine Laboratory, 375 Victoria Road, Aberdeen AB11 9DB, UK

c: Centre for Ecological and Evolutionary Synthesis (CEES), Department of Biosciences, University of Oslo, PO Box 1066 Blindern, N-0316 Oslo, Norway

d: Institute of Marine Research, Flødevigen, N-4817 His, Norway

e: University of Agder, Department of Natural Sciences N4604 Kristiansand, Norway

f: LARSyS – Associated Laboratory & Centre of IMAR of the University of the Azores, Department of Oceanography and Fisheries, 9901-862 Horta, Azores, Portugal.

g: School of Environment & Life Sciences, The University of Salford, Greater Manchester M5 4WT, UK

* Corresponding author: c.longmore@hotmail.com

Abstract

As human exploration and harvesting moves to the high seas, ecological understanding of the deep-sea has become a priority, especially in those commercially exploited species whose life cycle, habitat use and demographic structure remain poorly understood.

Here we combine otolith trace element and stable isotope analyses with microsatellite data to investigate population structure and connectivity in the migratory deep-sea black scabbardfish, *Aphanopus carbo*, sampled along a latitudinal gradient spanning much of the known species range in the north-east Atlantic.

In each sampled life stage, otolith trace element and oxygen isotope compositions are similar between fish from different capture locations, but otolith compositions vary greatly between life stages. Oxygen isotope compositions indicate ontogenetic migrations from relatively warm water conditions during larval growth to cooler waters with increasing age. Analysis of microsatellite DNA also suggests lack of genetic structure between the areas sampled.

The multidisciplinary approach employed collectively suggests that *A. carbo* individuals undergo an ocean-scale ontogenetic migration, beginning with spawning in southern, warm water Macaronesian areas (potentially dominated by Madeira), followed by a large proportion of immature fish moving to and feeding on the continental slope in northern areas.

The results lend the first conclusive evidence for defining the life-history circuit of this species and the perception of its stock structure across the north Atlantic.

43 **Keywords:** Deep-sea ecology, population structure, habitat use, otolith microchemistry,
44 stable isotope analysis, stock identification.

Introduction

For most deep-sea fish, there is rather limited information on general ecology, life cycles and population structure (Begg et al. 1999). In particular, the extent of large-scale migrations in deep-sea fish has not been well documented (Beamish et al. 2005), mainly due to the challenges associated with sampling and tracking (Starr et al. 2000). Lack of data on fish life history and ecology is particularly concerning when species are commercially exploited, and managed on a stock-specific basis.

The assessment of stock structure in marine fish populations should take into account processes acting at different spatial and temporal scales, including larval transport, recruitment, feeding, spawning, adaptation and past geographic isolation (Begg and Waldman 1999, Waples and Gaggiotti 2006). Molecular genetics has been used successfully to define management units (Hauser and Carvalho 2008, Waples et al. 2008), however, when used in isolation, genetic methods can struggle to resolve local demographic and life-history patterns over ecological time scales (Lowe and Allendorf 2010). Complementary methods exploit variation in the physiological and chemical make-up of an individual, providing insight into patterns of spatial structuring over time scales relevant to individual movements (Begg et al. 2005). Two such methods employ trace element concentrations and stable isotopes in the otolith as natural tags (Campana 2005, Elsdon et al. 2008).

Trace element analysis of otoliths for stock discrimination is based on the incorporation of minor and trace elements from the surrounding waters in the metabolically inert otolith, which becomes a permanent record of the chemical characteristics of the environment inhabited by the fish (Elsdon and Gillanders 2003, Stransky et al. 2005 Sturrock et al., 2012). Thus, the chronological properties of the

69 otolith can also be exploited by conducting spatially and temporally resolved chemical
70 analyses, effectively producing a record of variation in water chemistry experienced
71 throughout the entire life of the sampled individual. From this information it is possible
72 to infer location, migration, spawning events and habitat use (Campana et al. 1994,
73 Sturrock et al., 2012). Similarly, the stable oxygen isotope composition of the otolith
74 (commonly expressed as $\delta^{18}O$ values) preserves an indirect record of ambient water
75 temperature and salinity, and thus depth inhabited by the fish throughout its life (Kalish
76 1991, Hoie et al. 2004, Sherwood and Rose 2003, Thorrold et al. 1997). Consequently,
77 the isotopic composition of otolith aragonite can be employed to reveal temperature-
78 related aspects of fish location retrospectively and thus infer ontogenetic migratory
79 behaviour (Ashford and Jones 2007, Longmore et al. 2011, Rooker et al. 2008, Trueman
80 et al. 2012).

81 Recent studies in the North Atlantic suggest that otolith microchemistry can be
82 an effective tool in detecting patterns of spatial and temporal stock structuring in deep-
83 sea species (Shephard et al., 2007, Carlsson et al., 2011, Longmore et al. 2011), which
84 can complement and add insights to population genetic data (Knutsen et al. 2012).
85 While several previous studies have used various combinations of genetic, trace
86 element and stable isotope data to infer movements or stock structure (e.g. Smith and
87 Campana, 2010; Carlsson et al., 2011, Longmore et al. 2011), we know of no studies that
88 have combined employed genetic, trace elements and stable isotope analyses on the
89 same individual fish to infer movements and stock structure. The use of natural
90 markers such as otolith trace elements, stable isotopes and multi-locus genotypes can
91 provide a wealth of information spanning different temporal scales. The trace element
92 composition of otolith aragonite is influenced both by the fish's surrounding

93 environment and physiology (Elsdon et al. 2008, Sturrock et al. 2012). As the otolith is
94 an incremental structure, spatially resolved sampling provides a record of individual
95 movements and life history over the lifetime of an individual fish.

96 Genotypic markers on the other hand, are inherited and do not change during an
97 individual's life, so genotypic variation accumulates over several generations as a result
98 of microevolutionary forces (Lowe and Allendorf 2010). Genetic divergence in deep sea
99 fishes is generally low or nearly absent, e.g. the slender armourhead *Pseudopentaceros*
100 *wheeleri* (Martin et al. 1992), wreckfish *Polyprion americanus* (Ball et al. 2000) and the
101 alfonsino *Beryx splendens* (Akimoto et al. 2006). However, although most deep sea fish
102 display low values of genetic divergence, some do display significant genetic structure,
103 like the roundnose grenadier *Coryphaenoides rupestris* (Knutsen et al. 2012) and
104 bluemouth *Helicolenus dactylopterus (*Aboim 2005*).* Genetic structure in deep sea fishes
105 may also reveal cryptic patterns. For example no evidence of population structure could
106 be found in the orange roughy (*Hoplostethus atlanticus*) in the North Atlantic (White et
107 al. 2009). This was suggestive of high dispersal of adults which may not show any
108 homing behaviour but aggregate for spawning as the cause of a panmictic population.
109 However, Carlsson et al. (2011) recently identified fine scale population structure in
110 *Hoplostethus atlanticus* between raised and flat regions of the Porcupine Slope,
111 corresponding to differences in behaviour inferred from otolith stable isotope analyses.

112 Used in tandem, otolith and genetic markers can provide complementary
113 information, which may give a deeper insight into the stock structure, movement and
114 lifecycle of fish. Here, our aim is to assess population structure and test migratory
115 hypotheses in the black scabbardfish, *Aphanopus carbo* (Lowe, 1839); a deep-sea
116 predatory fish of significant commercial importance (approximately 7000 tonnes in

117 European waters in the last decade (ICES, 2008)).

118 *A. carbo* has a wide distribution across the North Atlantic, recorded on both sides
119 of the Atlantic. It occurs only sporadically north of the Scotland-Iceland-Greenland
120 ridges. In the North Atlantic it inhabits the continental slopes, seamounts and ridges,
121 between 200 and 1800m depth (Nakamura and Parin 1993). The early life stages of *A.*
122 *carbo* are assumed to be mesopelagic (Nakamura and Parin 1993), with a lifestyle that
123 becomes more benthopelagic as the fish grows, with vertical feeding migrations
124 reported at night (Merrett and Haedrich 1997). In the North Atlantic, *A. carbo* spawns
125 between the Macaronesian islands of Madeira (Figueiredo et al. 2003, Neves et al.
126 2009), the Canaries (Pajuelo et al. 2008) and, as recently found, the Azores (Stefanni,
127 pers. obs.). Generally, specimens caught in this area are larger, with all stages of
128 maturity represented, whereas the majority of fish found in more northern areas are
129 immature or in a post spawning state; in Rockall and around North-western Scotland, *A.*
130 *carbo* are smaller (61-117cm) (Figueiredo et al. 2003) and immature (Anon 2000, Kelly
131 et al. 1998).

132 Despite the uncertainties about population biology, the fishery in the NE Atlantic
133 is currently managed as two separate stocks, one in the south (ICES sub-area IX) and
134 one in the north (ICES sub-areas V, VI, VII and XII), although this is presently being
135 reconsidered (ICES 2012). It has been hypothesized that *A. carbo* in the North-east
136 Atlantic may comprise one single stock, with a southern spawning area (around
137 Madeira and the Canary islands) and a northern feeding ground (Swan et al. 2003),
138 connected by large scale migrations (Figueiredo et al. 2003). Such a hypothesis implies
139 an extensive migration across the NE Atlantic that could potentially cross a variety of
140 water masses with different physicochemical properties (Barbero et al. 2010, van Aken

141 2000). Indeed, the salinity and temperature regime differs significantly from warm
142 southern regions (Madeira, Azores, Portugal slope) to that of cold Northern areas
143 (Rockall). Southern localities are particularly susceptible to the outflow of high salinity
144 Mediterranean water, whereas Rockall is influenced by the North Atlantic current and
145 waters originating in the Labrador sea (Paillet at al 1998).

146 Studies of genetic structure of *A. carbo* populations are presently either
147 inconclusive (Quinta et al. 2004) or focused on phylogeographic history (Stefanni and
148 Knutsen 2007), and recent multidisciplinary efforts to discriminate individuals
149 recovered from different areas focused only on the southern north east Atlantic (Gordo
150 et al. 2009). Therefore, the specific aims of this study were to: i) assess the patterns of
151 area and habitat use across the life cycle of *A. carbo*, using otolith chemistry; ii) use
152 genotypic data to extrapolate the long-term connectivity implications of the
153 reconstructed life-history strategy; iii) Use collective evidence to reappraise the
154 population structure in this oceanic species.

155

Materials and Methods

Sampling and laboratory procedures

Black scabbardfish (*Aphanopus carbo*) were collected from seven locations across the North Atlantic: Rockall (including the Anton Dohrn Seamount), the western Irish Slope, the Hebridean Shelf, the Bay of Biscay, Madeira, the Azores and the Portuguese slope off Sesimbra, (Fig.1, Table. 1). All fish from Rockall, Anton Dohrn, Irish Slope, Hebrides and Bay of Biscay, were caught by bottom trawling and therefore from approximately 5 m above the seabed. Fish from the three southern locations were caught by long-line.

All fish ranged in size from 63 to 135 cm total length (TL). Maturity was assessed by gonad visual assessment, with maturity level assigned on a scale of 1-5 (0: immature 1: resting, 2: developing, 3: mature, 4: Spawning, 5: post spawning) (Figueiredo et al. 2003). All fish were measured to the nearest 0.5 cm (TL), weighed to the nearest 1 g, and otoliths collected on board from the Rockall, Madeira, Azores, and Portuguese Slope areas..

For DNA isolation, white skeletal muscle or gill tissue was taken from fresh specimens and either preserved in 96% ethanol at sea, or newly caught fish were frozen immediately on board the ship and, subsequently prepared in the laboratory.

Trace element analyses

Between 23 and 25 individuals per location were randomly selected (over all years sampled) for otolith trace element analysis. Before elemental analysis, otoliths

178 were weighed using a Mettler Toledo microbalance to the nearest 0.001 g. Elemental
179 data were acquired using a New Wave UP193FX (Electro Scientific Industries Europe
180 Ltd, Cambridge, UK) laser ablation system coupled to a Thermo Scientific X-Series II
181 ICP-MS (Thermo Scientific, Bremen, Germany). The following element/isotopes were
182 quantified: ^{7}Li, ^{24}Mg, ^{43}Ca, ^{44}Ca, ^{55}Mn, ^{59}Co, ^{60}Ni, ^{65}Cu, ^{66}Zn, ^{88}Sr, ^{137}Ba, ^{238}U. The analysis
183 parameters were as follows: spot size: 35 μm, pulse rate: 20 Hz, energy: 60%
184 (optimised), sweeps: 105, channels per mass: 1, channel: 0.02amu, acquisition time: 20
185 seconds, dwell time: 10ms, "wash" time between shots: 40 seconds. Standard reference
186 materials SRM 612 and SRM 610 produced by the National Institute of Standards and
187 Technology (NIST) were used for calibration and to monitor reproducibility. All data
188 were internally normalised to counts on ^{44}Ca to control for variable ablation efficiency
189 between otolith regions with relatively high and low organic contents. ^{43}Ca counts were
190 used as a post-normalization check. Typical LODs were as follows: ^{7}Li (3.53), ^{24}Mg
191 (3.62), ^{43}Ca, ^{44}Ca (705.39), ^{55}Mn (12.57), ^{59}Co (0.72), ^{60}NI (1.16), ^{65}Cu (1.89), ^{66}Zn (5.05),
192 ^{88}Sr (0.20), ^{137}Ba (0.60), ^{238}U (0.01).

193 A line of spots method was used to ablate each otolith, bisecting the annuli from
194 primordium to the edge (late adult stage) of the otolith to form a life history transect
195 (Supplementary material: Fig. S1.1). Following analysis, the laser pits were then
196 assigned to a life history stage based on otolith increment analyses (Morales-Nin et al.
197 2002). Laser pits were assigned to primordium (early larval), core (late larval),
198 transition (juvenile – end of year 1), and edge (late adult) stages. Fish from Rockall were
199 significantly younger (and smaller) overall than those captured from all other locations,
200 with their otolith radii on average approximately 80% of the size of those from the
201 other three locations. Therefore, the outer-edge data of Rockall fish were considered to
202 be representative of a "mid-life" life stage. To provide a comparison between fish caught

in Rockall and fish of a similar age and size caught in Azores, Madeira and Portugal slope areas, the radii of all otoliths were measured. A zone encompassing 80% +/-10% of the length of each otolith radius was identified and the laser shots within this zone were averaged for each fish to achieve a "mid-life" value comparable to otolith edge in fish caught in Rockall. For other life stages, the elemental concentrations from all spots falling within each designated life stage area in the otolith were averaged (Supplementary material: Fig. S1.1). The last three spots at the edge of each otolith in the Azores, Madeira and Portugal slope were thought representative of the latest adult phase (covering approx. 1-2 annuli) and the most recent environment inhabited by each fish and the last three spots of Rockall fish thought representative of a mid-life value.

Stable isotope analyses

From each area, five fish sampled for both genetic and trace element data were chosen randomly, and otoliths analysed for stable isotope compositions. Aragonite powder was micromilled from three regions, representing the core, mid and edge of the otolith representing larval, mid-life and late adult stages of life (Supplementary material: Fig. S1.1.). Stable isotope analyses were performed on a Geo Instruments mass spectrometer at the University of Southampton following the procedure detailed in Longmore et al. (2011). Analytical errors (standard error on repeat analyses of standards) were < 0.1‰ for both $\delta^{13}C$ and $\delta^{18}O$ values.

Data analysis and statistical methods

Initial screening of trace element data and statistical analysis closely follow those

227 of Longmore et al. (2011). Elements found to be correlated with each other were
228 included in further multivariate analyses but were subject to strict tolerance limits
229 (Berk 1977), which measures multicollinearity within the model (Tabachnick and Fidell
230 2001). Ba/Ca values were found to be correlated with otolith weight; however, the
231 slope of the relationship between otolith weight and the elemental concentration did
232 not vary among locations and so this was adjusted for by subtracting the product of
233 otolith weight and the common within-group slope from the elemental concentration
234 (DeVries et al. 2002, Tuset et al. 2006).

235 A initial 'repeated measures' ANOVA approach (Chambers and Miller 1995)
236 was used to account for non-independence of transect data sampled within each otolith
237 for both microchemical and isotope data and to test in an easily interpreted approach
238 whether the mean elemental and isotope ratios differed among sampling locations and
239 between designated life stage data. Further details of the repeated measures analysis
240 can be found in the supplementary material.

241 Based on overall chemical values, a stepwise discriminant function analysis
242 (DFA) of the element/Ca ratios for each life stage was used to assess the ability of
243 otolith trace element chemistry to assign individuals to the area of origin at each point
244 in their life. The DFA was jack-knifed to determine the discrimination success between
245 the sample areas using SYSTAT 8 (SYSTAT Software, 2002). Scatterplots of the first two
246 canonical variable scores were then drawn to visualize this separation.

247 Linear mixed effects models using data from all laser spots were used to
248 compare ontogenetic trends in the elemental concentration of otoliths from the four
249 sample locations, and to explore the effect of environmental (location) and biological
250 influences (age, sex, distance from core) on the ontogenetic element patterns. The

relationship between element/Ca ratios and otolith distances approximates a logarithmic trend, so element/Ca ratios were $\log_{10}$ transformed and linear mixed effects models (lme4 package in R) fitted to partition variance in ontogenetic patterns to specific physiological and environmental variables.

Initially, for each elemental response variable, a 'global model' was built (equation 1), including all single fixed effects and their first order interactions (indicated by the "*" command below). Categorical factor variables are underlined.

(1) $(E/Ca) = f(D_P + \underline{Loc} + \underline{LS} + \underline{S} + (D_P * Loc) + (D_P * LS) + (D_P * S) + (Loc * LS) + Loc * S) + (LS * S))$

where E/Ca is element/Ca, D_P is distance from primordium, Loc is location caught, LS is life stage and S is sex.

Fish identity was coded as a random effect to account for non-independence and autocorrelation of the response variables (element/Ca). Models were run using the maximum likelihood (ML) method, and optimal models indicated by stepwise removal of variables and interaction terms, with model performance assessed through Akaike information criterion (AIC) values (Crawley 2007). The performance of the final model was assessed through residuals analysis including normality, homogeneity and autocorrelation.

Reconstructing depth from otolith stable isotope data

Following methods in Shepherd et al (2007); Longmore et al (2011) and Trueman et al (2013), depth profiles of water temperature and salinity for each

sampled location were recovered from the BODC data repository. Profiles of otolith oxygen isotope ($\delta^{18}O_{oto}$) values expected at given depths were calculated using the algebraic relationships between temperature, salinity and otolith oxygen isotopes specifically adapted for deep water fishes (Longmore et al 2011, Trueman et al 2013). Measured $\delta^{18}O_{oto}$ values were compared to the corresponding $\delta^{18}O_{oto}$ profiles to estimate likely water depths (see Supplementary material: Fig. S1.2).

Genetic analyses

Genomic DNA isolation and screening of 11 microsatellite loci was carried out on a total of 651 individuals from seven sample locations, following published protocols. Some individuals failed to satisfactorily amplify at several loci and were considered to be partly degraded. For this reason, we elected to exclude all individuals from further considerations that failed at four or more loci. Due to the closely related, and morphologically similar, *A. intermedius* coexisting with *A. carbo* in the southern part of the study area, we screened the Azores and Madeira samples with species diagnostic mtDNA RFLP primers (Stefanni et al. 2009) and excluded all individuals identified as *A. intermedius.*

Population substructure in *A. carbo* was quantified by average F_{ST} over the 11 microsatellite loci (with 95% confidence limits calculated by jackknifing over loci), and tested for with log-likelihood allele frequency heterogeneity tests ("exact G-test" in GENEPOP '007). Robustness of genetic divergence (F_{ST}) estimates to potential confounding factors, including genotype scoring errors and intermixing with *A. intermedius* in the samples, was evaluated by linear regression of deviations from

297 expected (under Hardy-Weinberg equilibrium) genotype proportions (estimated by
298 Wright's fixation index, F_{IS}) on estimated F_{ST} within loci. Genetic similarities among
299 individuals and population samples were visualized by Principal Component Analysis
300 (PCA) and plotted in the multivariate space identified by the first two eigenvectors.

301

302 **Integration of microchemical and genetic data: a combined approach**

303 Between 23 and 25 individuals from Rockall, the Azores, Madeira and Portugal
304 slope had both otolith trace element and genotypic information. For these individuals,
305 all otolith and genetic markers were combined and analysed together to aid in the stock
306 discrimination process. As otolith and genetic data represent different temporal scales,
307 the chemistry for the pre-hatching/early larval stage was chosen for inclusion because
308 in a migratory species such as *A. carbo*, the earliest life stage should most closely
309 approximate the breeding population in the sample area.

310 Firstly a PCA using a correlation matrix was used to represent data with all
311 variables included. In total, 88 individuals with multi-marker information were
312 examined. Secondly, a non-parametric analysis of similarities, ANOSIM (Clarke 1993),
313 was then performed using the program PAST v1.89 (Hammer et al. 2001) to test for the
314 differentiation among the sampled groups. The ANOSIM rank-orders the values of a
315 distance matrix among all observations (in our case, the Euclidean distance among
316 individuals) and derives an R statistic, which expresses the ratio between the mean
317 rank of between-group (Rb) and within-group (Rw) distances. To test for the
318 significance of positive values of R, the observed value is compared to the 95%
319 confidence interval of a simulated distribution (in our case generated through 10,000

randomisations). R values were also generated and tested for significance for each pairwise comparison.

In addition, a Bayesian classification approach designed to combine different information types (Smith and Campana 2010) was applied to perform a stock classification simultaneously using the otolith mid-life trace element and genetic data. The Bayesian framework developed by Smith and Campana (2010) (performed using R and WINBUGS via the mixFish package) classifies a mixed population of unknown origin into one of several base populations of known origin (and the parameter values of the classified mixed samples are also used to refine the classification). In the case of *A. carbo*, we expect (based on previous data analysis) that there is a strong migratory component to the stock, and thus expect to find no distinct structure between the baseline populations, and poor classification. Non-informative priors were used for otolith element means, and pseudo-Bayes estimates of informative priors used for allele frequencies as described in Smith and Campana (2010). We set the juvenile aggregation in Rockall as the mixed sample to be partitioned among the Azores, Madeira and Portugal slope potential spawning areas.

Results

Otolith chemical life-history reconstruction

Single element values

Overall differences in mean elemental ratios among locations were not significant but all were highly significant between life stages (Table S1.1). Untransformed elemental ratios averaged by life stage and location can be viewed in the Supplementary material: Table S1.2.

Although not showing significant overall differences, some elemental ratios showed some variation among locations at each life stage. Within the primordial zone of the otolith (representing the prehatching/early larval phase), the Zn/Ca and Ba/Ca ratios differed most among locations (Fig. 2). Microchemical analysis of the late larval (core) zone of the otolith found that only Zn/Ca was variable between sample locations (Fig. 2). Variations among locations in the transitional zone of the otoliths were found for the Li/Ca, Mn/Ca and Ba/Ca ratios. Adult region (edge) microchemistry of the otolith revealed that the ratios Zn/Ca, and Ba/Ca were most variable among locations. Although a weak pattern of elemental variability among some pairs of locations at each life stage was found, ontogenetic changes in chemistry within locations were much more pronounced (Fig. 2), particularly for Li/Ca, Mn/Ca and Zn/Ca ratios, with values decreasing gradually from early larval to transitional phases with a large decrease into the adult stages. Details of variation in all elements/Ca ratios between sample locations and life stages can be found in the Supplementary material: Table S1.1 and Table S1.2.

357 *Overall spatial and temporal patterns in otolith chemistry*

358 Based on initial overall patterns of spatial variation in elemental concentration
359 among locations, the ratios Li/Ca, Mn/Ca, Zn/Ca and Ba/Ca were chosen for preliminary
360 inclusion in the DFA. The elemental ratios contributing most to classification differed
361 depending on life stage. The DFA of early larval stage otolith chemistry was mostly
362 driven by Li/Ca, Zn/Ca and Ba/Ca, and gave an overall jack-knifed classification success
363 of 41% (Fig. 3). For core (late larval) otolith data, the overall jack-knifed classification
364 success was also 41%, with Zn/Ca and Ba/Ca values contributing most to the
365 classification. For the transitional phase, classification success was 40%, with Li/Ca and
366 Ba/Ca values contributing most to classification (see Supplementary material: Table
367 S1.3). A 42% classification was found at the late adult stage, with highest classification
368 in Rockall (57%) and lowest in the Azores (21%)(Fig. 3). As Rockall individuals are
369 considerably smaller than the other three locations, their "late adult" stage (otolith
370 edge) would correspond to a "mid-life" range in fish from the other three locations.
371 However, Rockall individuals were included in the "late adult" DFA as the edge
372 chemistry represents the most recent environment of the fish and so would be useful to
373 assess assignment of individuals to the area of origin based on area specific chemistry.

374 Linear mixed effect models were carried out to examine which physiological
375 and/or environmental variables best explained ontogenetic variations in otolith
376 element concentrations, using fish identity as a random effect. For each element, a
377 model of element/Ca ratio as a function of linear distance from the otolith core was built
378 for all fish. Residuals for each model were evenly spread but frequently departed from
379 normality. This was a reflection of the relatively constant and high values of most
380 element/Ca ratios in the otolith cores. Li/Ca, Zn/Ca, and Cu/Ca varied from primordium

381 to otolith edge indicating strong ontogenetic influences on otolith chemistry
382 (Supplementary material: Fig S1.3-1.5). All ratios showed high concentrations in the
383 core, followed by a prominent decrease and eventual stabilization in concentration with
384 distance from the primordium (age). Sr/Ca values in all locations showed a similar
385 pattern of an initial decrease in ratio values up to ~400-600 μm (age 1-2) from the
386 primordium, which was followed by consistent, gradual increases in ratio values. Ba/Ca
387 values show a gradual decline in early life (Fig. S1.5) up to approximately 700 μm from
388 the primordium (age 2-3). Elemental profiles from all locations then show a
389 stabilization of Ba/Ca followed a gradual increase in concentration after mid life and
390 into the adult life stage. The linear mixed model identified location and sex as important
391 variables influencing ontogenetic patterns in Li/Ca, Zn/Ca, and Cu/Ca.

392 Ontogenetic trends in Mg/Ca and Mn/Ca ratios are summarized in Fig. 4, as these
393 ratios in particular showed evidence for variable life-history trends in Madeiran fish.
394 The ontogenetic pattern of Mg/Ca values in fish from Madeira is extremely variable in
395 early life with concentrations spanning the range from the other three locations (Fig. 4).
396 Mg/Ca values are relatively stable in individual otoliths over the main portion of life but
397 between-individual variance is greater in otoliths collected from Madeira than from the
398 other three locations (Mg/Ca SD (μmol mol^{-1}): Rockall = 5.6, Madeira = 6.1, Azores = 4.6,
399 Portugal slope = 3.2 (Fig. 4). Location contributed to variance in ontogenetic patterns in
400 the mixed model analyses, but no influence of sex was detected on Mg/Ca values. Again
401 adult fish recovered from Madeira showed more variability in Mn/Ca values in early life
402 stages than fish collected from any of the other locations (Fig. 4). Location and sex were
403 identified as variables that were strongly influencing ontogenetic patterns in Mn/Ca
404 values.

405 ***Oxygen Isotope Analysis: water temperature reconstruction***

406 Individuals from all locations show a common ontogenetic pattern of increasing
407 $\delta^{18}O_{oto}$ values with age (Fig. 5, Supplementary material: Table S1.4). $\delta^{18}O$ values indicate
408 an average equivalent temperature of 13 (± 1) °C in the larval phase, 11.5 (± 1) °C in
409 mid-life and 9 (± 1) °C in the adult stage. Among locations, there was no significant
410 difference in $\delta^{18}O$ values with the adjusted alpha of 0.005 (repeated measures ANOVA, F
411 (3, 5) = 0.361, p = 0.78). Between life stages, differences were highly significant
412 (repeated measures ANOVA, F (1.34, 6.7) = 21.03, p = 0.002).

413 Fish caught in the Rockall area show $\delta^{18}O_{oto}$ values corresponding to
414 surrounding waters of 14 (± 1), 11 (± 1) and 10 (± 1) °C for early life stage, mid-life and
415 adult phases respectively (Fig. 5). Estimated ontogenetic ambient water temperatures
416 for fish caught on the Portuguese slope range from 13 (± 1), 12 (± 1) and 11 (± 1) ºC,
417 while for the Azores were 13 (± 1), 11 (± 1) and 6 (± 1) °C for early life stage, mid-life
418 and adult phases respectively. Recovered values for Madeiran fish were 13 (± 1), 10 (±
419 1) and 8 (± 1) °C for early life stage, mid-life and adult phases.

420

421

422 **Genetic Structure**

423

424 The 11 microsatellite loci uncovered a near absence of genetic population
425 structure over the sample area. The average F_{ST} over loci across the four focal locations
426 was just 0.0004 with a 95% confidence interval (CI) of -0.0006 to 0.0013, thus broadly
427 overlapping zero. Including additional samples (and pooling the two replicate Rockall
428 samples) did not modify the overall picture of low spatial divergence, and average F_{ST}
429 increased only marginally, to 0.0008 (95%CI: 0.0000 to 0.0015). No connection was
430 found between deviations from Hardy-Weinberg genotype proportions (F_{IS}: data not
431 shown) and F_{ST} among samples (linear regression, $R^2 = 0.055$, P = 0.49), nor when
432 comparing F_{IS} within *A. carbo* to F_{ST} beween *A. carbo* and *A. intermedius* ($R^2 = 0.0013$, P
433 = 0.55), indicating robustness of our estimates to potential genotyping errors (null
434 alleles and allele drop-out) and/or intermixing of species (Wahlund effect).

435 Considering pairs of samples, only the Azores-Madeira pair displayed a nominal
436 statistically significant difference, however with a very low estimate of F_{ST} between
437 them (0.0017: Table 2). Nine of the 28 (i.e, a third) pairwise F_{ST} estimates were zero or
438 negative, and indicating an absence of genetic divergence among the samples. The
439 remaining estimates were positive (range 0.0001 to 0.0043) and several of these must
440 be judged statistically significant, also after applying the False Discovery Rate correction
441 (Benjamini & Hochberg 1995). The temporal replicate samples from Rockall (ROC) were
442 not different from each other, giving some indication of temporal stability at least over
443 the short term (3 years).

444 PCA ordination of samples from the four focal locations (422 individuals, Fig. 6A)

445 and all locations (Fig. 6B) provided a picture of remarkable overlap among genotype
446 distributions, with virtually no appreciable differences among locations.

447

448 **Integration of otolith-genetic data: a combined approach**

449 Examining the PCA ordination of combined otolith-genetic data from the four
450 focal locations, it is clear that the general trend of overlapping variance is maintained
451 (Fig. 6C). The ANOSIM results (Table 3.) show that between-group variance is not
452 significantly greater than the within-group variance (hence an R-value close to zero).
453 Pairwise comparisons had no significant results, indicating lack of differentiation among
454 sample locations based on this multi-marker approach. The Bayesian analysis similarly
455 yielded poor classification success: using otolith element data alone, 75% credible
456 intervals on the posterior estimates of group proportions overlap, indicating a lack of
457 elemental differentiation between potential base populations. Using either the genetic
458 data or a combined approach, there is some suggestion of differentiation between the
459 Portugal slope (Sesimbra) and Macaronesian samples, but 95% credible intervals
460 overlap, again suggesting that any apparent distinction between populations is poorly
461 supported (Fig S1.6).

462 All variables (alleles or elements) for which more than 5 individuals had missing
463 data were removed, and any individuals with further missing data were also removed.
464 Therefore the Bayesian analysis had a sample of 11 fish from Azores, 14 from Madeira
465 and 22 from the Portugal slope (Sesimbra). It should be noted that the fact that
466 Sesimbra appears potentially more similar to Rockall than the others (genetically) may
467 reflect this differing sample size (especially as assigned individuals from the mix case
468 are used to define the characters of the base populations within the Bayesian method.

469

Discussion

Otolith microchemistry: Reconstructing patterns of area and habitat use

At all life stages, a strong overlap in otolith elemental composition was evident across locations. This suggests either overall panmixia in this highly mobile deep-sea species or that the physicochemical environments of these locations are similar. The former is more likely as it has been shown that the more southern locations of this study differ significantly in temperature and salinity (which affect elemental uptake) to that of the Northern location (Ellett and Martin 1973, van Aken 2000). Similarly, the stable physico-chemical water parameters of the deep-sea (Pörtner et al. 2004) and the large geographic range of samples presumes greater variation in water chemistry among locations than from year to year. Thus, differences in otolith chemistry among years of capture should be relatively stable, as it was indeed detectable in another deep sea species with a similar distribution range (Longmore et al. 2011). A similar study of the otolith microchemistry of the macrourid fish, *C. rupestris*, from four locations in the NE Atlantic (two of which broadly correspond to two of the focal locations investigated here) demonstrated strong location-specific variation in otolith chemistry at all life stages (Longmore et al. 2011). Furthermore, in the present study, oxygen isotopic values recovered for the larval portion of otoliths from *A. carbo* caught at Rockall appear to correspond to water temperatures that are nearly twice as high as those typical of the Rockall area, suggesting that Northern fish caught in Rockall have a larval phase in southern (warmer) waters. This indicates that a significant number of juvenile *A. carbo* make a northerly migration from southern waters. What was not clear, however, is whether any of the adult *A. carbo* sampled in Maderian waters had migrated back from Rockall; their isotopic and elemental signatures were simply indistinguishable from all

494 areas.

495 The strong influence of life stage on element patterns suggests common
496 ontogenetic changes in either physiology or ambient water chemistry. All elements
497 showed significant ontogenetic changes in chemistry (Supplementary material: Figs
498 S1.3-1.5) with a general pattern of a longitudinal decrease in elemental ratios.
499 Ontogenetic physiological influences are likely to be responsible for changes in
500 elemental ratios such as Mg/Ca (Sturrock 2012), but currently the influence of
501 physiological processes on trace element partitioning throughout ontogeny is not fully
502 understood.

503 Some elemental profiles reveal trends that may be related to variation in life
504 history trajectories. Mn/Ca and especially Mg/Ca identify the Madeiran fish as having
505 unusually varied concentrations in the larval/early juvenile portion of otoliths. This
506 variability appears to stabilize at the same period as fish from the other three locations
507 (Fig. 4). This may be indicative of Madeira containing fish that were spawned in a
508 variety of locations. Therefore Madeiran waters may not only act as a source in the NE
509 Atlantic as a major spawning site, it may also be a sink for individuals from other
510 spawning aggregations. The pattern of otolith microchemistry observed reflects
511 ontogenetic migrations both laterally and vertically. Based on the consistent
512 ontogenetic increase in $\delta^{18}O_{oto}$ values in all locations, fish from all regions appear to be
513 migrating to deeper waters at similar times, thus the highly variable chemistry in
514 Madeiran fish in particular is more likely to reflect a degree of lateral migratory
515 behaviour. However, the possibility of a more complex water column around Madeira
516 may also play a role (van Aken 2000).

517

518 *Reconstructing a life-history circuit*

519 Previous studies have suggested a single stock unit of *A. carbo* in the NE Atlantic,
520 with a spawning ground in the south (e.g. Madeira) and a sub-adult feeding ground in
521 the north (i.e. Rockall), but none were able to rigorously test the idea. Swan et al. (2003)
522 found small differences between the overall chemical values of the otoliths from these
523 study areas. A study on the reproductive cycle of *A. carbo* in the NE Atlantic showed that
524 the largest specimens caught were from Madeira, where all stages of maturity were
525 present, and the smallest specimens were found in the Rockall region (Figueiredo et al.
526 2003). This length separation between North and South was also found by a similar
527 separate study with an expanded length dataset (Carvalho and Figueiredo 2001).
528 Furthermore, life circuit continuity between North and South was inferred based on the
529 gonadal maturation cycle (Santos et al. 2013).

530 The hypothesis of a life history migration of *A. carbo* with a southern spawning
531 ground (Madeira, Azores and Canaries area) and a Northern feeding ground (Rockall
532 region) (Figueiredo et al. 2003) was supported by a number of results achieved by this
533 study. Examining the DFA results in more detail, classification accuracy in the Madeira
534 sample increased gradually from 45% in the primordium, to 71% in the transitional
535 phase, indicating that a large proportion of fish stay resident in this area in early life.
536 However, in the adult phase, classification accuracy decreased to a minimum (38%).
537 This further supports the view that Madeiran waters contain a mix of fish from several
538 locations at the adult stage, indicating partial migration, whereby both migratory and
539 resident individuals (Chapman et al. 2012) can be found in what probably represents a
540 critical spawning ground for the species. Although not reflected in the DFA results, *A.*
541 *carbo* has been reported to be present all year round in the Azores suggesting there are

542 also resident fish around this location (Stefanni, pers. obs.). Comparing the early-stage
543 elemental and isotope values from all sample locations revealed an indistinguishable
544 chemistry. Although this suggests that all fish hatched in a similar environment, it is not
545 possible to infer whether they all effectively hatched around Madeira, or rather some
546 were spawned somewhere else that had similar environmental conditions.

547 The $\delta^{18}O$ data recovered also provided valuable information on the movements
548 and habitat use of this species. In situ average sea water temperatures for the capture
549 depth (and years) of fish at each location also matched the recovered temperature
550 estimates from $\delta^{18}O_{oto}$ values to within 2°C. Oxygen shows a common life-history trend
551 in all locations from warmer waters (shallow) in core regions (<2 years) to colder
552 waters (deeper) in later life. In the NE Atlantic, temperature varies significantly with
553 depth (van Aken 2000) and the changes in temperature observed throughout the
554 lifecycle of *A. carbo* most likely reflect a vertical depth migration. As stressed above,
555 $\delta^{18}O_{oto}$ values recovered for the larval portion of otoliths from fish caught in Rockall
556 correspond to high water temperatures, consistent with a southerly origin. This
557 indicates that *A. carbo* makes a northerly (feeding) migration from southern waters
558 before the onset of maturity.

559

560 *Long-term connectivity implications of the reconstructed life-history strategy*

561 Genetic data suggested an absence of population structure across most of the
562 distribution area of this species, indicating that the life cycle of this species may be
563 conducive to panmixia. Microsatellite DNA results were congruent with the findings
564 from trace elements and isotope analysis in indicating a lack of substructure, and

absence of distinct biological populations. While low levels of genetic divergence are sometimes associated with distinct biological populations (Knutsen et al. 2011, Ryman et al. 1979), the present estimate (F_{ST} = 0.0008 or lower) is at least an order of magnitude lower still, and its confidence interval overlap zero. In simplified theoretical models (Wright's island model), this level of divergence (or lack thereof) indicates that putative populations are effectively exchanging several hundred or more individuals per generation (Waples and Gaggiotti 2006). Closer inspection of table 3 indicates that genetic differences, if any, follow a complex pattern. There was little agreement among methods (F_{ST} or G-test) as to which pairs that differ (indicated by asterisks in table 2), and only three "significant" pairs are in common between methods. Two of these pairs involve the HE sample, and because this sample is quite old (year 1999), we cannot exclude the possibility that it reflects temporal, rather than spatial, divergence.

We find no consistent, significant pattern of spatial genetic divergence among samples of *A. carbo* covering most of its distribution range in the eastern and middle North Atlantic. Based on lines of evidence from otolith chemistry, we are inclined to believe that this reflects lack of phylopatry, and a migratory/dispersal strategy that guarantees re-mixing of genotypes over generations

The very subtle signal of F_{ST} = 0.0017 between Madeira and the Azores might underlie the existence of isolated pockets of independent spawning aggregations further away from Madeira. However, collective, multidisciplinary evidence indicates that the large scale feeding migrations of *A. carbo* result in demographic mixing across generations, with younger cohorts returning from northern areas without natal homing, and with the Madeiran aggregation being composed of individuals likely hatched in different southern areas of the north Atlantic. Such diversity of individual life history

589 trajectories may function as an 'adaptive insurance' on fitness, much in the way that has
590 been proposed for some well-studied stocks of coastal/shelf species (McQuinn 1997).

591

592 *Reappraisal of the perceived population structure in A. carbo*

593 Our study is the first time that both otolith chemistry and population genetics
594 have been used to test the hypotheses regarding stock structure and the migratory cycle
595 of *A. carbo*. Individually, the analyses of otolith microchemistry and genetics (alone or
596 combined in a multi-marker framework) revealed a lack of any
597 differentiation/structure in *A. carbo* recovered from distinct locations over the North-
598 East Atlantic. Otolith stable isotopes revealed the existence of southern origin for *A.*
599 *carbo* recovered in Rockall, strongly suggesting that at least a proportion of the
600 population for this species is migratory. In agreement with other work (Figueiredo et al.
601 2003, Santos et al. 2013, Swan et al. 2003), this multidisciplinary study is suggestive of
602 large-scale migration in the NE Atlantic, resulting in functional near-panmixia in the
603 black scabbardfish *A. carbo*.

604 Current fisheries management considers the *A. carbo* stock in the NE Atlantic as
605 comprised of two components (North and South), but the findings of this study suggest
606 that assessing Rockall and Macaronesian fisheries separately may be biologically
607 unjustified, primarily because northern fish are originated from a southerly spawning
608 stock. However, we cannot rule out the existence of hitherto unrecognized complexities
609 in other spawning aggregations, especially the southerly aggregation in the Canary
610 Islands (Pajuelo et al. 2008). The recent finding of spatial overlap in southern Azorean
611 waters, between *A. carbo* and its more southerly sister species, *A. intermedius* (Stefanni

612 and Knutsen 2007), leaves open possibilities to yet more discoveries on this taxon.

613

614 **Acknowledgements**

615 Part of this study includes work from C.L's PhD studies, financially supported by the
616 European Science Foundation (EuroDEEP), the Irish Research Council and the MARECO
617 network. We are very grateful to all scientific and commercial fishing expeditions that
618 provided samples, including cruises by Scottish, Irish, Portuguese and Norwegian crews.
619 We would like to thank Gui Menezes (DOP) and the research project PESCPROF, project
620 co-financed by EU Interreg III B program who generously donated otolith samples from
621 the Azores. S.S. is a researcher contracted by IMAR/DOP under the "Ciência 2007"
622 recruitment program funded by FCT (Foundation for Science and Technology, Portugal).
623 We are especially grateful to all members of the DEECON project (www.imr.no/deecon)
624 for the many fruitful discussions on life history of *A. carbo*. Finally, we would also like to
625 thank the two reviewers and subject editor for their valuable and constructive criticism.

626

627

628 **References**

629 Aboim MA, Menezes GM, Schlitt T, Rogers AD (2005) Genetic structure and history of
630 populations of the deep-sea fish Helicolenus dactylopterus (Delaroche, 1809)
631 inferred from mtDNA sequence analysis. Molecular Ecology, 14, 1343–1354
632 Akimoto S., Itoi S., Sezaki K., Borsa P., Watabe S. 2006. Identification of alfonsino Beryx
633 mollis and B. splendens collected in Japan, based on the mitochondrial
634 cytochrome b gene, and their comparison with those collected in New Caledonia.
635 Fish Sci, 72, 202–207.
636 Anon, M.S. 2000. Final report of the EU study project CT 97/0084 Environment and
637 biology of deep-water species Aphanopus carbo in NE Atlantic: basis for its
638 management (BASBLACK). DGXIV European commission.
639 Ashford, J., and Jones, C. 2007. Oxygen and carbon stable isotopes in otoliths record
640 spatial isolation of Patagonian toothfish (*Dissostichus eleginoides*). Geochim.
641 Cosmochim. Acta 71(1): 87-94.
642 Ball, A.O., Sedberry, G.R., Zatcoff, M.S., Chapman, R.W., and Carlin, J.L. 2000. Population
643 structure of the wreckfish Polyprion americanus determined with microsatellite
644 genetic markers. Mar Biol 137(5-6): 1077-1090.
645 Barbero, L., González-Dávila, M., Santana-Casiano, J.M., and Álvarez, M. 2010. Variability
646 of the water mass transports and fluxes in the eastern North Atlantic during
647 2001. J. Geophys. Res. 115(C3): C03023.
648 Beamish, R.J., McFarlane, G.A., and King, J.R. 2005. Migratory patterns of pelagic fishes
649 and possible linkages between open ocean and coastal ecosystems off the Pacific
650 coast of North America. Deep Sea Res. Part II 52(5-6): 739-755.
651 Begg, G.A., Campana, S.E., Fowler, A.J., and Suthers, I.M. 2005. Otolith research and

652 application: current directions in innovation and implementation. Mar.
653 Freshwater Res. 56(5): 477-483.
654 Begg, G.A., Friedland, K.D., and Pearce, J.B. 1999. Stock identification and its role in stock
655 assessment and fisheries management: an overview. Fish. Res. 43(1-3): 1-8.
656 Begg, G.A., and Waldman, J.R. 1999. An holistic approach to fish stock identification.
657 Fish. Res. 43(1-3): 35-44.
658 Benjamini, Y. & Hochberg, Y. (1995) Controlling the false discovery rate: a practical and
659 powerful approach to multiple testing. J. R. Stat. Soc., Series B, 289-300.
660 Berk, K.N. 1977. Tolerance and Condition in Regression Computations. J. Am. Stat. Assoc.
661 72(360a): 863-866.
662 Campana, S.E. 2005. Otolith science entering the 21st century. Mar. Freshwater Res.
663 56(5): 485-495.
664 Campana, S.E., Fowler, A.J., and Jones, C.M. 1994. Otolith Elemental Fingerprinting For
665 Stock Identification of Atlantic Cod (*Gadus Morhua*) Using Laser-Ablation Icpms.
666 Can. J. Fish. Aquat.Sci. 51(9): 1942-1950.
667 Carlsson, J., Shephard, S., Coughlan, J., Trueman, C.N., Rogan, E., Cross, TF. 2011 Fine
668 scale population structure in a deep-sea telesot (orange roughy Hoplostethus
669 atlanticus). Deep Sea Res. 1 58, 627-636.
670 Carvalho, M.L., and Figueiredo, I. 2001. Establishing a sampling programme for
671 monitoring changes in the length distribution of the black scabbardfish
672 (*Aphanopus carbo* Lowe, 1839) in the Northern Atlantic Ocean. In Proceedings of
673 the Advanced Workshop on Environmental Sampling and Monitoring, 22–24
674 March, Estoril, Portugal.
675 Chambers, R.C., and Miller, T.J. 1995. Evaluating fish growth by means of otolith

676 increment analysis: special properties of individual-level longitudinal data. pp.
677 155-175, In, Recent developments in fish otolith research. D. H. Secor, J. M. Dean,
678 and S. E. Campana, editors. University of South Carolina Press, Columbia, SC 764
679 p.
680 Chapman, B.B., Skov, C., Hulthén, K., Brodersen, J., Nilsson, P.A., Hansson, L.A., and
681 Brönmark, C. 2012. Partial migration in fishes: definitions, methodologies and
682 taxonomic distribution. J. Fish Biol. 81(2): 479-499.
683 Clarke, K.R. 1993. Non-parametric multivariate analysis of changes in community
684 structure. Austral. Ecol. 18: 117–143.
685 Crawley, M.J. (2007) The R Book. — John Wiley & Sons Ltd
686 DeVries, D.A., Grimes, C.B., and Prager, M.H. 2002. Using otolith shape analysis to
687 distinguish eastern Gulf of Mexico and Atlantic Ocean stocks of king mackerel.
688 Fish. Res. 57(1): 51-62.
689 Ellett, D.J., and Martin, J.H.A. 1973. The physical and chemical oceanography of the
690 Rockall channel. Deep Sea Res. 20: 585-625.
691 Elsdon, T.S., and Gillanders, B.M. 2003. Reconstructing migratory patterns of fish based
692 on environmental influences on otolith chemistry. Rev. Fish. Biol. Fisher. 13(3):
693 217-235.
694 Elsdon, T.S., Wells, B.K., Campana, S.E., Gillanders, B.M., Jones, C.M., Limburg, K.E., Secor,
695 D.H., Thorrold, S.R., and Walther, B.D. 2008. Otolith chemistry to describe
696 movements and life-history parameters of fishes: Hypotheses, assumptions,
697 limitations and inferences. Oceanogr. Mar. Biol., Annu. Rev. 46: 297.
698 Figueiredo, I., Bordalo-Machado, P., Reis, S., Sena-Carvalho, D., Blasdale, T., Newton, A.,
699 and Gordo, L.S. 2003. Observations on the reproductive cycle of the black
700 scabbardfish (*Aphanopus carbo* Lowe, 1839) in the NE Atlantic. ICES J. Mar. Sci.

701 60(4): 774-779.
702 Gordo, L.S., Baptista, I., Carvalho, L., Costa, V., Cruz, C., Eiras, J., Farias, I., Figueiredo, I.,
703 Lourenço, H., Bordalo-Machado, P., Neves, A., Nunes, M., Reis, S., Santos, M.,
704 Saraiva, A., and Vieira, A. 2009. Stock structure of black scabbardfish (*Aphanopus*
705 *carbo* Lowe, 1839) in the southern northeast Atlantic. Sci. Mar. 73(S2): 89-101
706 doi: 110.3989/scimar.2009.3973s2089
707 Hammer, Ø, Harper, D.A.T, Ryan, P.D. 2001. PAST. Paleontological Statistics Software
708 Package for Education and Data Analysis. *Palaeontol. Electronica* 4:
709 http://palaeo-electronica.org/2001_1/past/issue1_01.htm.
710 Hauser, L., and Carvalho, G.R. 2008. Paradigm shifts in marine fisheries genetics: ugly
711 hypotheses slain by beautiful facts. Fish and Fisheries 9(4): 333-362
712 Hauser, L., Seamons, T.R., Dauer, M., Naish, K.A., and Quinn, T.P. 2006. An empirical
713 verification of population assignment methods by marking and parentage data:
714 hatchery and wild steelhead (*Oncorhynchus mykiss*) in Forks Creek, Washington,
715 USA. Mol.Ecol. 15(11): 3157–3173Hauser, L., and Carvalho, G.R. 2008. Paradigm
716 shifts in marine fisheries genetics: ugly hypotheses slain by beautiful facts. Fish
717 Fish 9(4): 333-362
718 Hoie, H., Otterlei, E., and Folkvord, A. 2004. Temperature-dependent fractionation of
719 stable oxygen isotopes in otoliths of juvenile cod (*Gadus morhua* L.). ICES J. Mar.
720 Sci. 61(2): 243-251.
721 ICES WGDEEP Report 2008. Report of the Working Group on the Biology and
722 Assessment of Deep-sea Fisheries Resources (WGDEEP). ICES Advisory
723 Committee. ICES Headquarters, Copenhagen
724 ICES. 2012. Report of the Stock Identification Methods Working Group (SIMWG), 14 - 16

May 2012, Manchester, UK. . ICES CM 2012/SSGSUE:04: 48 pp.

Kalish, J.M. 1991. 13C and 18O isotopic disequilibria in fish otoliths – metabolic and kinetic effects. Mar. Ecol. Prog. Ser. 75: 191-203.

Kelly, C.J., Connolly, P.L., and Clarke, M.W. 1998. The deep water fisheries of the Rockall trough: some insights gleaned from Irish survey data. ICES CM 1998/O:40: 22 pp.

Knutsen, H., Catarino, D., Sannæs, H., and Stefanni, S. 2009. Development of eleven microsatellite loci in the deep-sea black scabbardfish (*Aphanopus carbo*). Conserv. Genet. Resour. 1(1): 89-92.

Knutsen, H., Jorde, P.E., Bergstad, O.A., and Skogen, M. 2012. Population genetic structure in a deepwater fish *Coryphaenoides rupestris*: patterns and processes. Mar. Ecol. Prog. Ser. 460: 233-246.

Knutsen, H., Olsen, E.M., Jorde, P.E., Espeland, S.H., AndrÉ, C., and Stenseth, N.C. 2011. Are low but statistically significant levels of genetic differentiation in marine fishes 'biologically meaningful'? A case study of coastal Atlantic cod. Mol. Ecol. 20(4): 768-783.

Longmore, C., Trueman, C., Neat, F., Gorman, E., Milton, J., and Mariani, S. 2011. Otolith geochemistry indicates life-long spatial population structuring in a deep-sea fish, *Coryphaenoides rupestris*. Mar. Ecol. Prog. Ser.435: 209-224.

Lowe, W.H., and Allendorf, F.W. 2010. What can genetics tell us about population connectivity? Mol. Ecol. 19(15): 3038-3051.Martin AP, Humphreys R, Palumbi SR (1992) Population geneticstructure of the armourhead, Pseudopentaceros wheeleri, in theNorth Pacific Ocean: application of the polymerase chain reactionto fisheries populations. Can. J. Fish. Aquat.Sci., 49, 2368–2391.

McQuinn, I.H. 1997. Metapopulations and the Atlantic herring. Rev. Fish. Biol. Fisher. 7(3): 297-329.

750 Merrett, N.R., and Haedrich, R.L. 1997. Deep-Sea Demersal Fish and Fisheries. Chapman
751 and Hall London: 282 pp.
752 Morales-Nin, B., Â. Canha, M. Casas, I. Figueiredo, L.S. Gordo, M. Gordon, E. Gouveia, C.G.
753 Piñeiro, S. Reis, A. Reis and S.C. Swan. – 2002. Intercalibration of age readings of
754 deepwater black scabbardfish, Aphanopus carbo (Lowe, 1839). ICES J. Mar. Sci.,
755 59: 352-364
756 Nakamura, I., and Parin, N.V. 1993. FAO species catalogue. Vol. 15. Snake mackerels and
757 cutlassfishes of the world (Families Gempylidae and Trichiuridae). An annotated
758 and illustrated catalogue of the snakemackerels, snoeks, escolars, gemfishes,
759 sackfishes, domine, oilfish, cutlassfishes, scabbardfishes, hairtails, and frostfishes
760 known to date. FAO Fisheries Synopis. No. 125 Vol. 15. : 1-136.
761 Neves, A., Vieira, A., Farias, I., Figueiredo, I., Sequeira, V., and Gordo, L.S. 2009.
762 Reproductive strategies in black scabbardfish (*Aphanopus carbo* Lowe, 1839)
763 from the NE Atlantic. Sci. Mar. 73 (S2): 19-31 doi:
764 10.3989/scimar.2009.3973s2019
765 Paillet, J., Arhan, M., and McCartney, M.S. 1998. Spreading of Labrador Sea Water in the
766 eastern North Atlantic. J. Geophys. Res. 103(C5): 10223-10239
767 Pajuelo, J.G., Gonzalez, J.A., Santana, J.I., Lorenzo, J.M., Garcia-Mederos, A., and Tuset, V.
768 2008. Biological parameters of the bathyal fish black scabbardfish (*Aphanopus*
769 *carbo* Lowe, 1839) off the Canary Islands, Central-east Atlantic. Fish. Res. 92(2-
770 3): 140-147.
771 Pörtner, H., Langenbuch, M., and Reipschläger, A. 2004. Biological Impact of Elevated
772 Ocean CO2 Concentrations: Lessons from Animal Physiology and Earth History. J.
773 Oceanogr. 60(4): 705-718.

774 Quinta, R., Gomes, L., and dos Santos, A.T. 2004. A mitochondrial DNA PCR-RFLP marker
775 for population studies of the black scabbardfish (*Aphanopus carbo*). ICES J. Mar.
776 Sci. 61(5): 864-867.
777 Rooker, J.R., Secor, D.H., DeMetrio, G., Kaufman, A.J., Belmonte Rios, A., and Tina, V. 2008.
778 Evidence of trans-Atlantic movement and natal homing of bluefin tuna from
779 stable isotopes in otoliths. Mar. Ecol. Prog. Ser. 368: 231-239.
780 Rousset, F. (2008) GENEPOP'007: a complete re-implementation of the GENEPOP
781 software for Windows and Linux. Mol. Ecol. Res., 8, 103-106
782 Ryman, N., Allendorf, F.W., and Ståhl, G. 1979. Reproductive isolation with little genetic
783 divergence in sympatric populations of brown trout (*Salmo trutta*). Genetics
784 92(1): 247-262.
785 Santos, A.R., Trueman, C., Connolly, P., and Rogan, E. 2013. Trophic ecology of black
786 scabbardfish, *Aphanopus carbo* in the NE Atlantic—Assessment through stomach
787 content and stable isotope analyses. Deep Sea Res. Part I 77(0): 1-10.
788 Shephard, S., Trueman, C., Rickaby, R., Rogan, E. 2007 Juvenile life history of NE Atlantic
789 orange roughy from otolith stable isotopes Deep Sea Res. 1- 54:1221-1230
790 Sherwood, G.D., and Rose, G.A. 2003. Influence of swimming form on otolith delta C-13
791 in marine fish. Mar. Ecol. Prog. Ser. 258: 283-289.
792 Smith, S.J. and Campana, S.E. 2010. Integrated stock mixture analysis for continuous and
793 categorical data, with application to genetic–otolith combinations. Can. J. Fish.
794 Aquat. Sci. 67:1533-1567.
795 Starr, R.M., Heine, J.N., and Johnson, K.A. 2000. Techniques for Tagging and Tracking
796 Deepwater Rockfishes. N. Am. J. Fish. Manage. 20(3): 597-609.
797 Stefanni, S., and Knutsen, H. 2007. Phylogeography and demographic history of the

798 deep-sea fish *Aphanopus carbo* (Lowe, 1839) in the NE Atlantic: Vicariance
799 followed by secondary contact or speciation? Mol. Phylogenet. Evol. 42(1): 38-
800 46.
801 Stransky, C., Garbe-Schonberg, C., and Gunther, D. 2005. Geographic variation and
802 juvenile migration in Atlantic redfish inferred from otolith microchemistry. Mar.
803 Freshwater Res. 56: 677–691.
804 Sturrock, A.M., Trueman, C.N., Darnaude, A.M. and Hunter, E. 2012. Can otolith
805 elemental chemistry retrospectively track migrations in fully marine fish?
806 *Journal of Fish Biology*. 81, 766-795.
807 Swan, S.C., Gordon, J.D.M., and Shimmield, T. 2003. Preliminary investigations on the
808 uses of otolith microchemistry for stock discrimination of the deep-water black
809 scabbardfish (*Aphanopus carbo*) in the North East Atlantic. J. Northwest Atl. Fish.
810 Soc. 31: 221-231.
811 Tabachnick, B.G., and Fidell, L.S. 2001. Using Multivariate Statistics. 4th ed. Boston,
812 Mass: Allyn and Bacon; 2001.
813 Thorrold, S.R., Campana, S.E., Jones, C.M., and Swart, P.K. 1997. Factors determining 13C
814 and 18O fractionation in aragonitic otoliths of marine fish. Geochim. Cosmochim.
815 Acta 61: 2909–2919.
816 Trueman, C.N., MacKenzie, K.M., and Palmer, M.R. 2012. Identifying migrations in
817 marine fishes through stable-isotope analysis. J. Fish Biol. 81(2): 826-847.
818 Trueman, C.N., Rickaby, R.E.M., and Shephard, S. 2013. Thermal, trophic and metabolic
819 life histories of inaccesible fishes revealed from stable isotope analyses. A case
820 study using orange roughy Hoplostethus atlanticus Collett 1889. J. Fish. Biol. *In*
821 *Press 2013.*

822 Tuset, V.M., Rosin, P.L., and Lombarte, A. 2006. Sagittal otolith shape used in the
823 identification of fishes of the genus *Serranus*. Fish. Res. 81(2-3): 316-325.
824 van Aken, H.M. 2000. The hydrography of the mid-latitude Northeast Atlantic Ocean II:
825 The intermediate water masses. Deep Sea Res. Part I 47(5): 789-824.
826 Waples, R.S., and Gaggiotti, O. 2006. What is a population? An empirical evaluation of
827 some genetic methods for identifying the number of gene pools and their degree
828 of connectivity. Mol. Ecol. 14: 1419-1439.
829 Waples, R.S., Punt, A.E., and Cope, J.M. 2008. Integrating genetic data into management
830 of marine resources: how can we do it better? Fish. Fish. 9(4): 423-449.
831 White, T.A., Stefanni, S., Stamford, J., and Hoelzel, A.R. 2009. Unexpected panmixia in a
832 long-lived, deep-sea fish with well-defined spawning habitat and relatively low
833 fecundity. Mol. Ecol. 18(12): 2563-2573
834
835

836 **Table 1.** Details of *A. carbo* samples used for both chemical and genetic analyses. Total
837 sample includes both otolith and genetic samples. TL stands for 'Total Length' and
838 represents TL for the total sample.

839 **Table 2**. Pairwise measure of differentiation among *A. carbo* samples. Below diagonal:
840 F_{ST} (asterisks indicate that the lower 5% confidence level was greater than zero). Above
841 diagonal: P-value for exact G tests on allele frequencies, summed over loci with Fisher's
842 method (asterisks indicate statistically significant at the 5% level or better under the
843 FDR approach to multiple testing's). AZO: Azores, MAD: Madeira, PTS: Portugal slope,
844 BB: Bay of Biscay, IRS: Irish slope, HE: Hebrides, ROC: Rockall.

845 **Table 3.** ANOSIM output for the four sample locations. Pairwise R-values below the
846 diagonal, p-values above. ANOSIM R: 0.023, Anosim P-value: 0.1 (within group variance
847 18.81, between group variance 1925).

848

849 **Table 1.**

Location	N (Otoliths)	N (Total)	Year	Depth (m)	TL (cm)	Sex ratio (F/M)
Rockall	23	163	2006/2008	750-850	42-108	2.7: 1
Madeira	23	91	2008	1100	106-135	3.5: 1
Azores	24	72	2002-2008	1115-1525	77-133	2.7: 1
Portugal slope	24	96	2008	800-1200	95-125	1.22: 1
Hebrides	0	60	1999	975-1420	80-117	-
Bay of Biscay	0	84	1999	1160	87-123	-
Irish slope	0	85	2006	-	72-115	-

850

851

852

853 **Table 2.**

Sample	AZO	MAD	PTS	BB	IRS	HE	ROC6	ROC8
AZO	-	0.0010*	0.3474	0.0009*	0.0001*	0.0019*	0.0121	0.0027
MAD	0.0017*	-	0.1172	0.1225	0.0001*	0.0009*	0.1748	0.0187
PTS	-0.0015	0.0004	-	0.1532	0.0415	0.0019	0.0902	0.2262
BB	0.0022	0.0012	0.0011	-	0.1908	0.0828	0.6177	0.0101
IRS	0.0013	0.0011	-0.0002	-0.0008	-	0.0000*	0.0914	0.0824
HE	0.0037*	0.0040*	0.0043*	-0.0002	0.0014	-	0.0171	0.0050
ROC6	0.0016	0.0005	0.0016	-0.0004	-0.0005	0.0021	-	0.0266
ROC8	0.0007	0.0000	-0.0004	0.0003	-0.0011	0.0017*	0.0001	-

854

855 **Table 3.**

	ROC	AZO	MAD	PTS
ROC	0	0.2241	0.6067	0.1295
MAD	0.0174	0	0.0675	0.2487
AZO	- 0.01457	0.05598	0	0.0714
PTS	0.0302	0.01291	0.04495	0

856

857

858 **Fig. 1.** Northeast Atlantic, showing study locations (Circles) where *A. carbo* were
859 sampled. ROC: Rockall, HE: Hebrides, IRS: Irish slope, BB: Bay of Biscay, PTS: Portugal
860 slope, MAD: Madeira, AZO: Azores.

861 **Fig. 2.** Mean elemental ratios (umol mol^{-1} Log_{10} transformed) and standard deviations
862 for *A. carbo* otoliths from each of four sample sites and life stages. Any locations not
863 sharing a common letter are significantly different from each other ($p < 0.005$).

864 **Fig. 3.** Ordination plots of *A. carbo* individuals using the first two canonical variates
865 extracted via stepwise discriminant function analysis of elemental ratios. Colour-coding
866 and shape identifies sampling locations. Ellipses are for visualization purposes only.
867 Abbreviations as in Figure 1. Early larval stage (a), Late larval stage (b), Transitional
868 stage (c) and Adult stage (d).

869 **Fig. 4.** Elemental profile of Mg/Ca and Mn/Ca as a function of distance from
870 Primordium. F: Female (Black), M: Male (Red).

871 **Fig. 5.** Mean Oxygen isotope (bars) per life stage with equivalent water temperature
872 (lines). (a) Rockall, (b) Madeira, (c) Azores and (d) Portugal slope.

873 **Fig. 6.** PCA ordinations of (a) genetic data for the four locations (including a temporal
874 repeat of Rockall) sharing otolith analyses. Colour-coding and shape identifies sampling
875 locations. Abbreviations as in Figure 1, (b) genetic data for all localities sampled. ROC:
876 Rockall, HE: Hebrides, IRS: Irish slope, BB: Bay of Biscay, PTS: Portugal slope, MAD:
877 Madeira, AZO: Azores. ROC – 08 and ROC – 06 are temporal repeats of the same locality
878 and (c) combined otolith and genetic data for the four focal locations. Colour-coding and
879 shape identifies sampling locations as in (a).

880 The following Supplementary material is available for this article online

881

882 **Table S1.1.** Repeated measures ANOVA (Greenhouse- Geisser) results of elemental
883 profiles across *A. carbo* otoliths collected at four locations across the NE Atlantic.
884 Bracketed numbers indicate degrees of freedom.

885 **Table S1.2** *Aphanopus carbo*. Mean untransformed concentrations and standard error
886 (in brackets) of trace elements standardised to Ca (μmol mol^{-1}) per sample location and
887 life stage.

888 **Table S1.3** Jack-knifed classification matrices for discriminant function analysis of early
889 larval (EL), late larval (LL), transition phase (T) and late adult (A) elemental ratios of *A.*
890 *carbo* among the four sites. Overall summary and relative proportions are reported in
891 the final eight columns.

892 **Table S1.4** Mean Oxygen and Carbon stable isotope values of *A. carbo* otoliths per
893 location. J: Juvenile, ML: Mid-Life, A: Adult. PTS: Portugal slope, MAD: Madeira, ROC:
894 Rockall and AZO: Azores.

895

896 **Fig. S1.1** *Aphanopus carbo* (Black scabbardfish) otoliths showing (Top image) otolith
897 microchemistry analysis zones corresponding to the Primordial zone (P) representing
898 the early larval phase, the core zone (C) representing the late larval phase, the
899 transitional zone (T), the mid-life zone (M – in otoliths from the Azores, Madeira and
900 Portugal slope) and the late adult phase (A – referred to as edge in the main
901 manuscript) representative of most recent environment of the fish. Lower image: otolith

902 isotope analysis zones (laser spots are for microchemistry only, not stable isotopes),
903 corresponding to the juvenile zone (J) encompassing early/late larval phases, the mid-
904 life stage (M) and the late adult phase (A), representative of most recent environment of
905 the fish.

906 **Fig. S1.2** Predicted otolith $\delta^{18}O$ ($\delta^{18}Ooto$) values calculated from CTD profiles of
907 temperature and salinity for four sample locations of *A. carbo* in the North Atlantic.

908 **Fig. S1.3** Elemental profile of Li/Ca as a function of distance from Primordium.

909 **Fig. S1.4** Elemental profile of Sr/Ca as a function of distance from Primordium.

910 **Fig. S1.5** Elemental profile of Ba/Ca as a function of distance from Primordium.

911 **Fig. S1.6** Bayesian posterior estimates of the proportional group membership for
912 Rockall juveniles (+75% credible intervals) using otolith only, genetic only or combined
913 data.

914

915

916

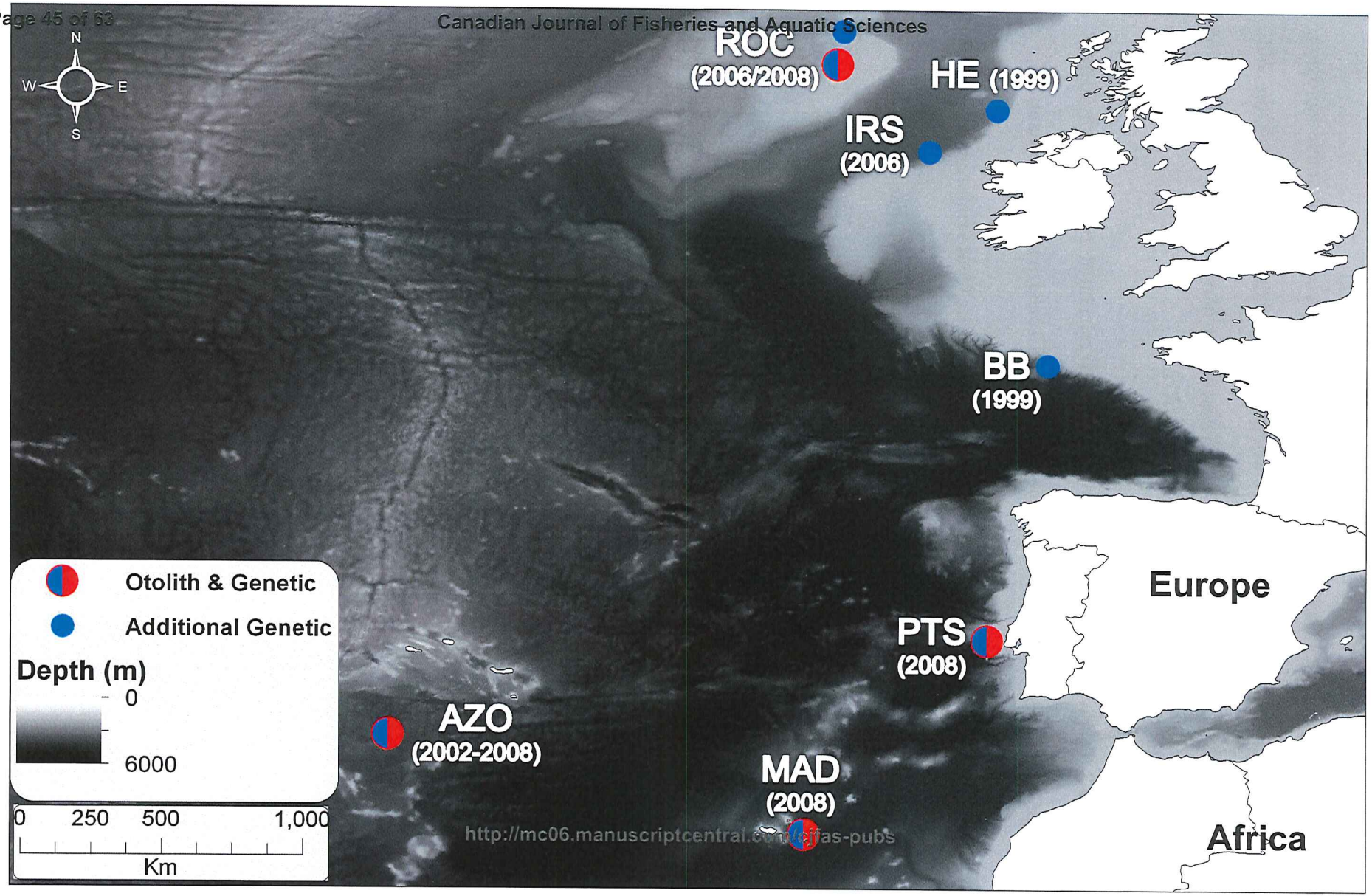

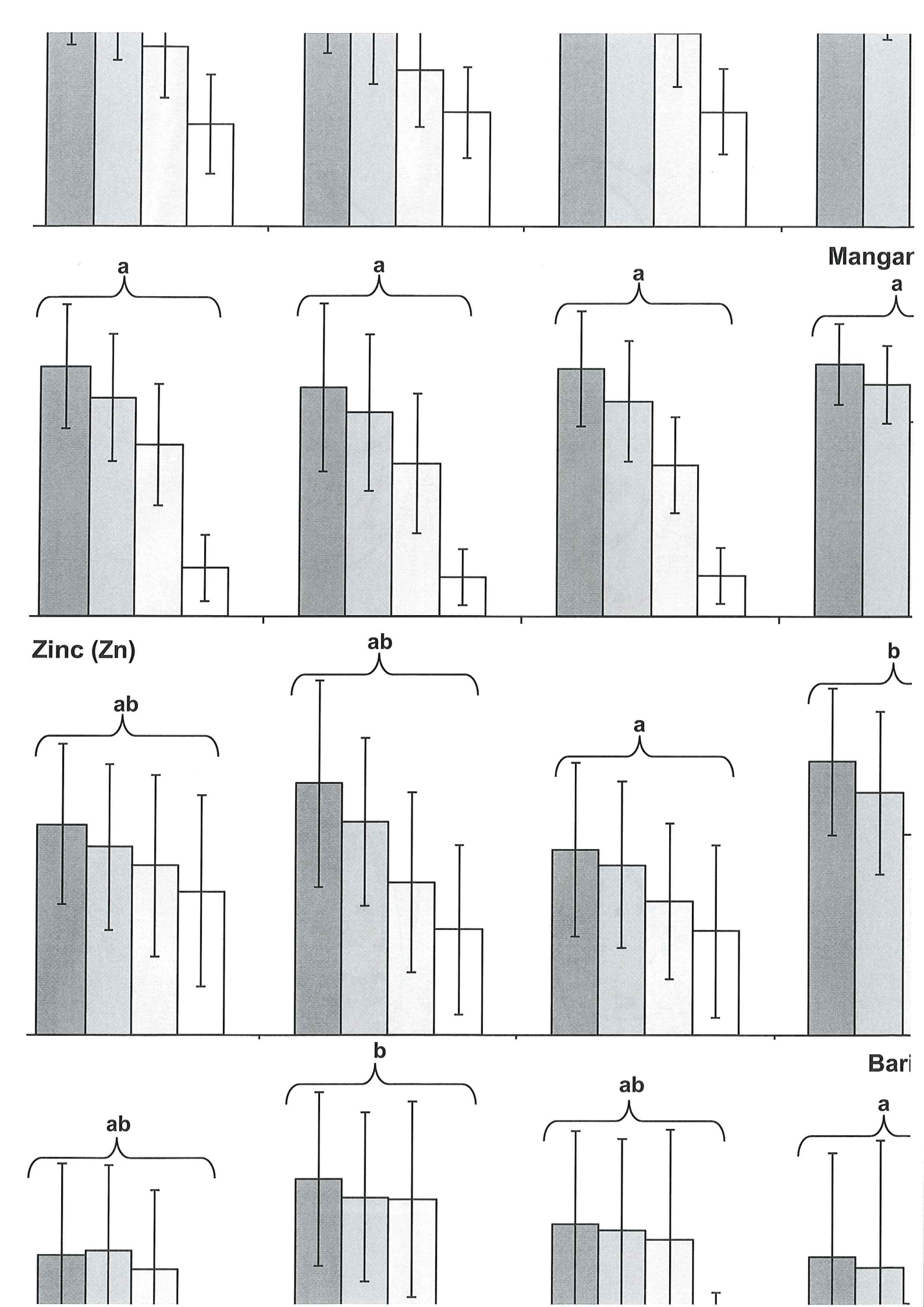
Mangar
Zinc (Zn)
Bari
a
a
a
a
ab
ab
a
b
ab
b
ab
a

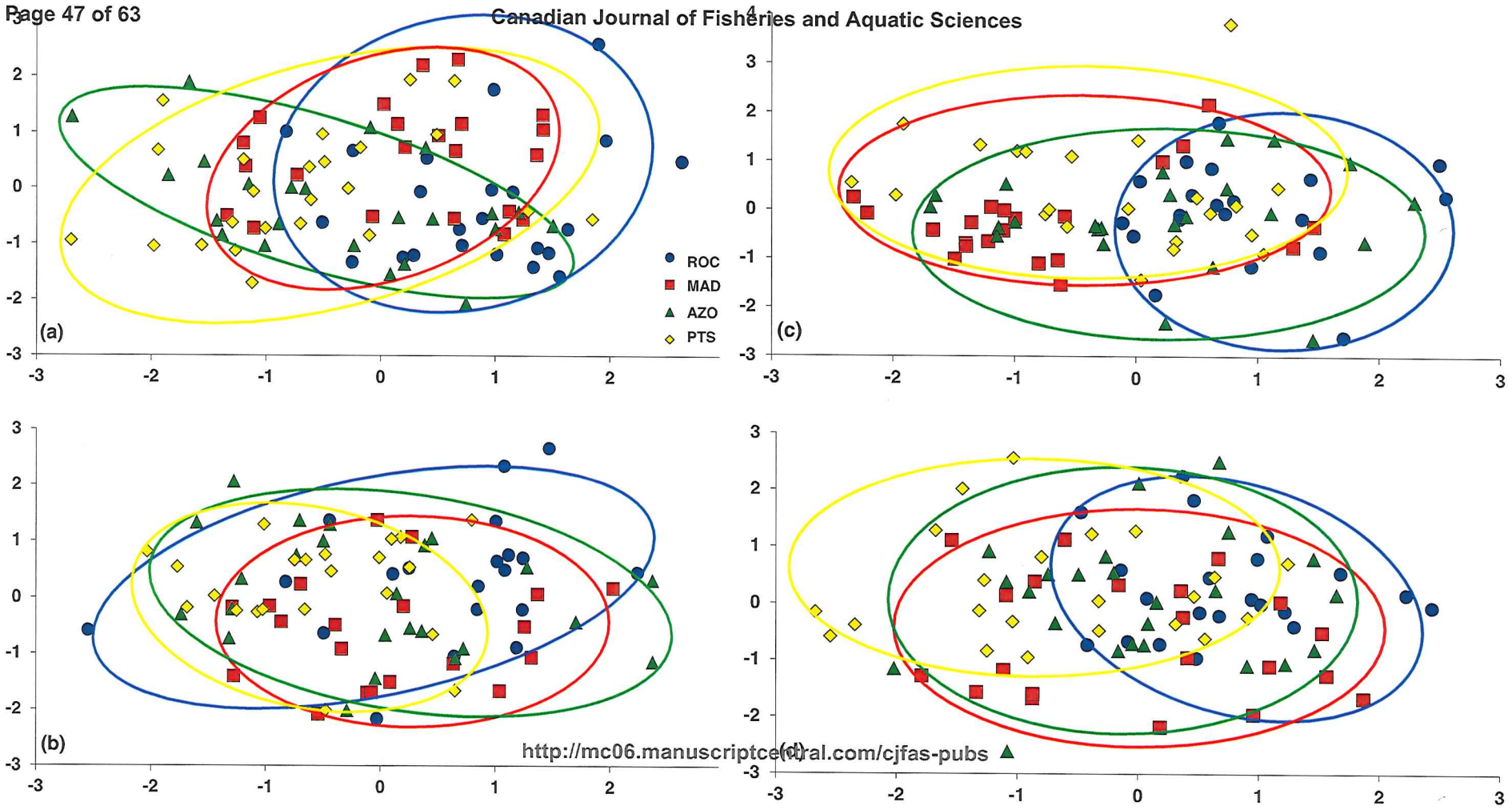

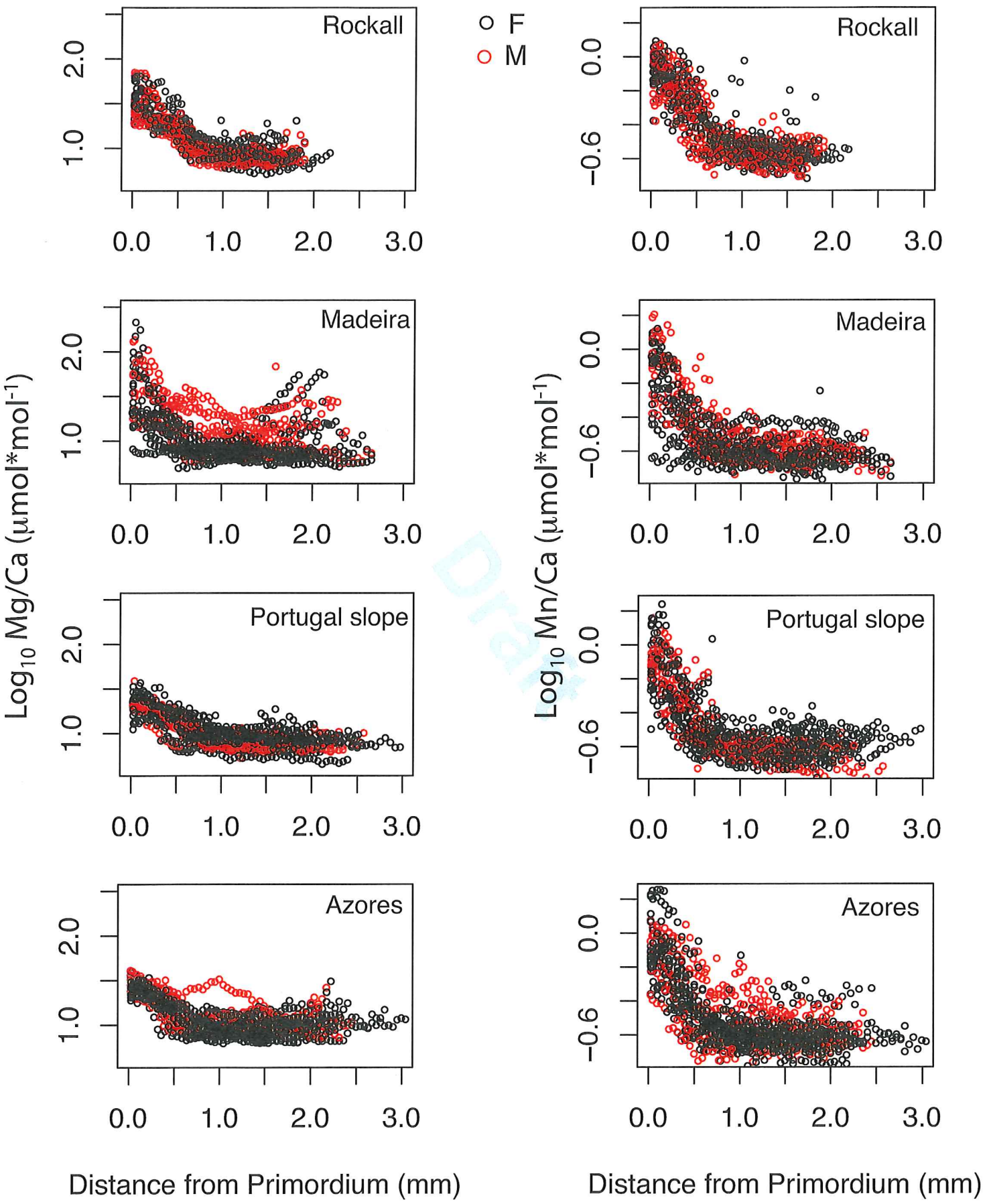
F
M
Rockall
Madeira
Portugal slope
Azores
Log10 Mg/Ca (µmol*mol-1)
Log10 Mn/Ca (µmol*mol-1)
Distance from Primordium (mm)
Distance from Primordium (mm)
1.0
2.0
0.0
1.0
2.0
3.0
−0.6
0.0

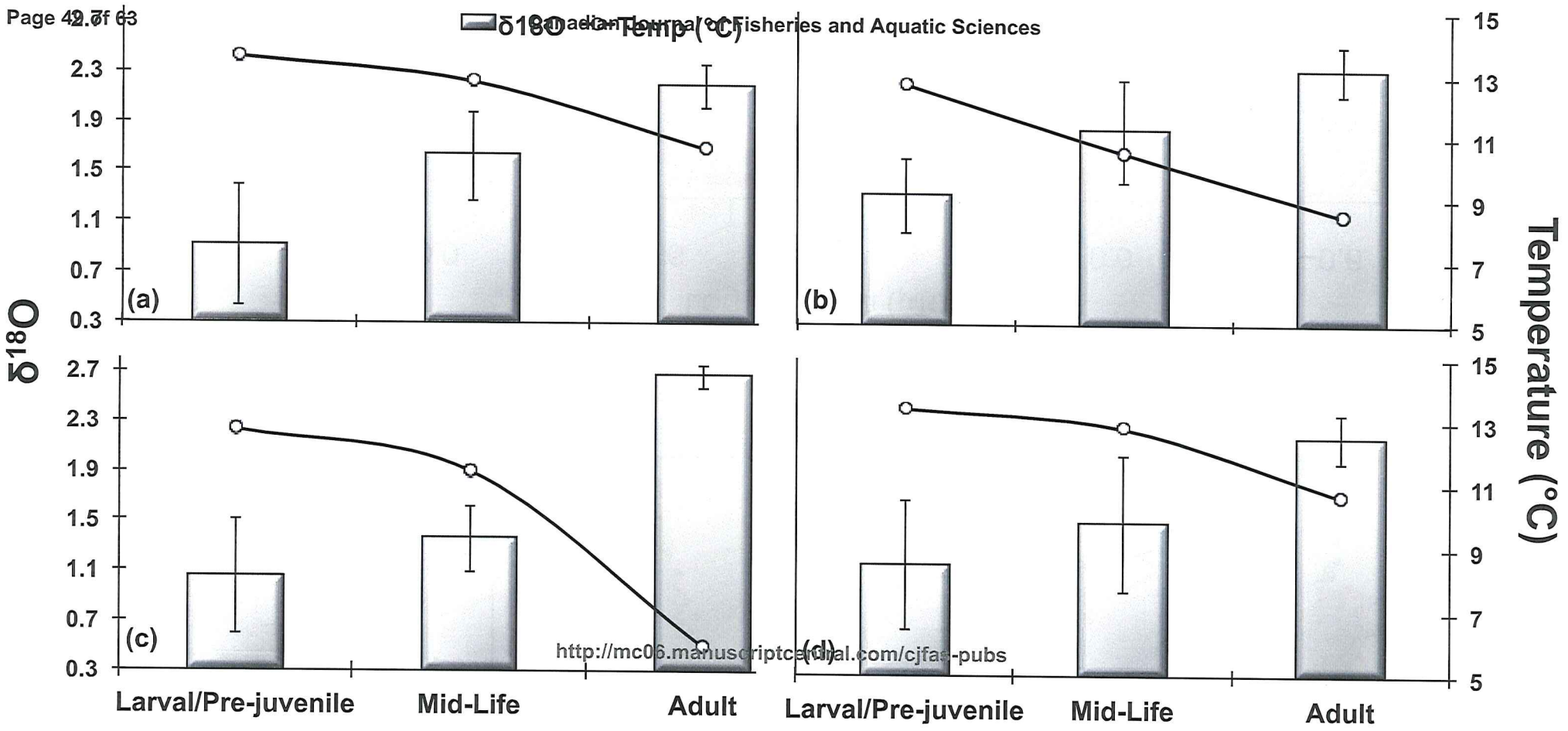

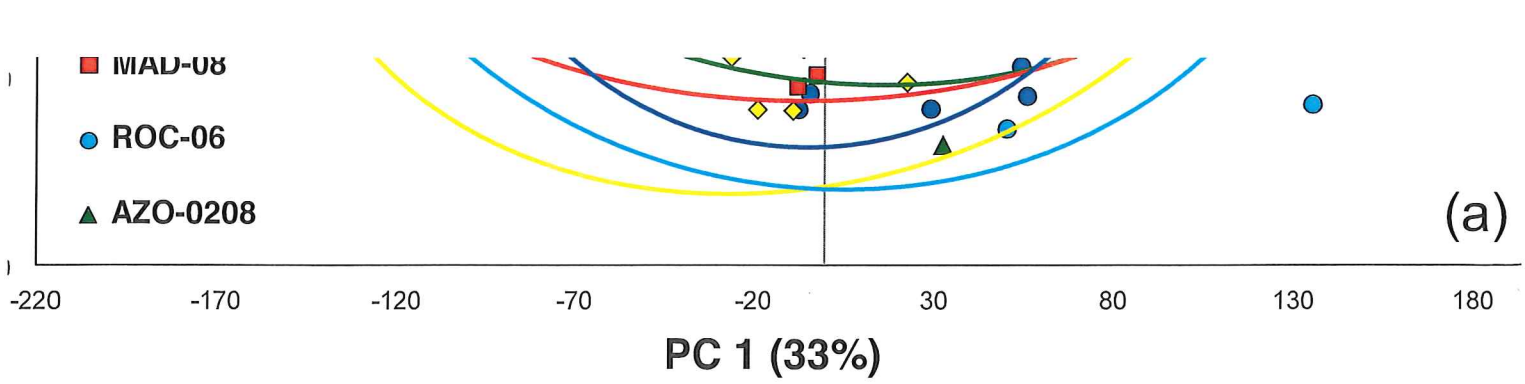
MAD-08
ROC-06
AZO-0208
(a)
-220
-170
-120
-70
-20
30
80
130
180
PC 1 (33%)

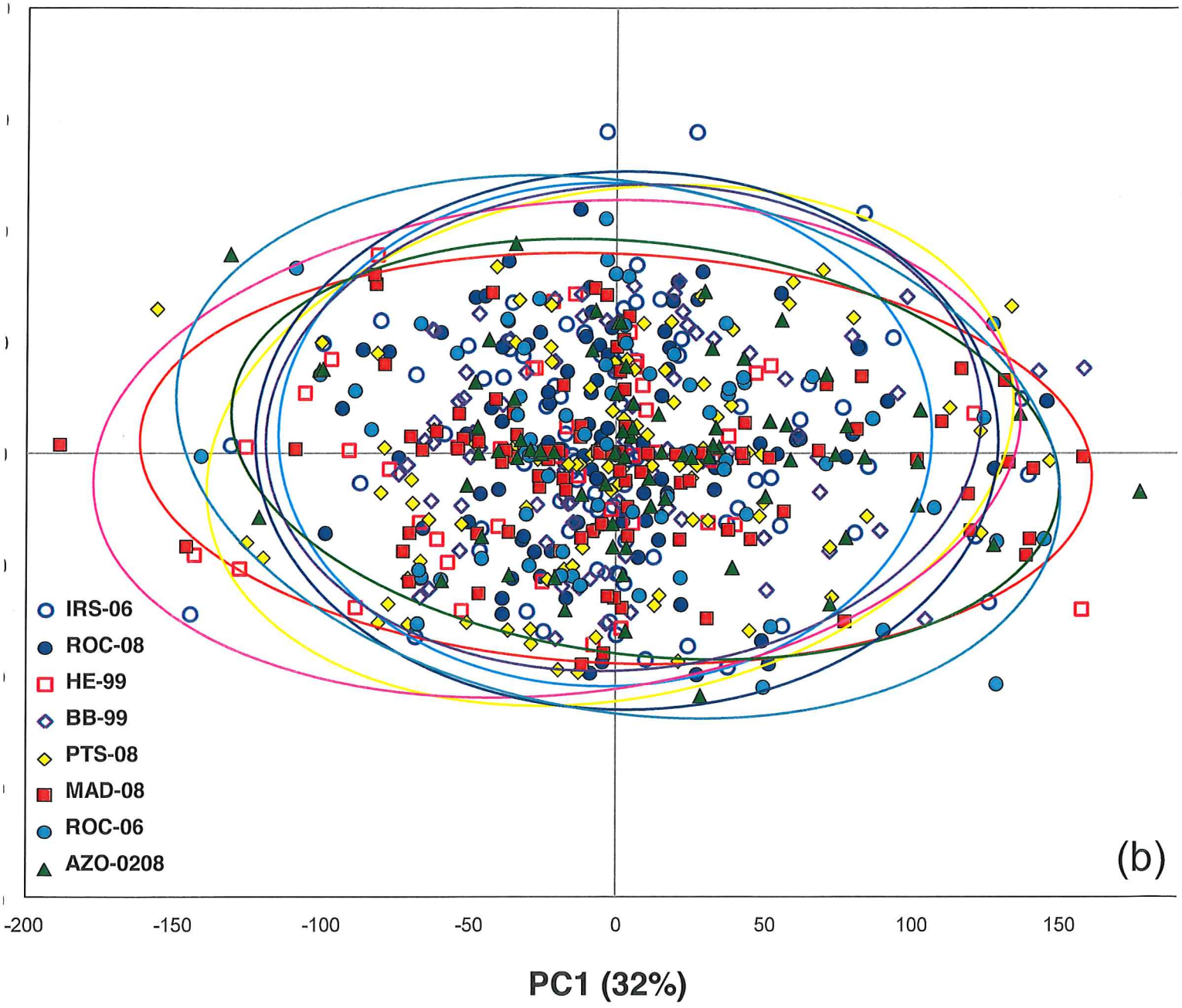
IRS-06
ROC-08
HE-99
BB-99
PTS-08
MAD-08
ROC-06
AZO-0208
(b)
-200
-150
-100
-50
0
50
100
150
PC1 (32%)

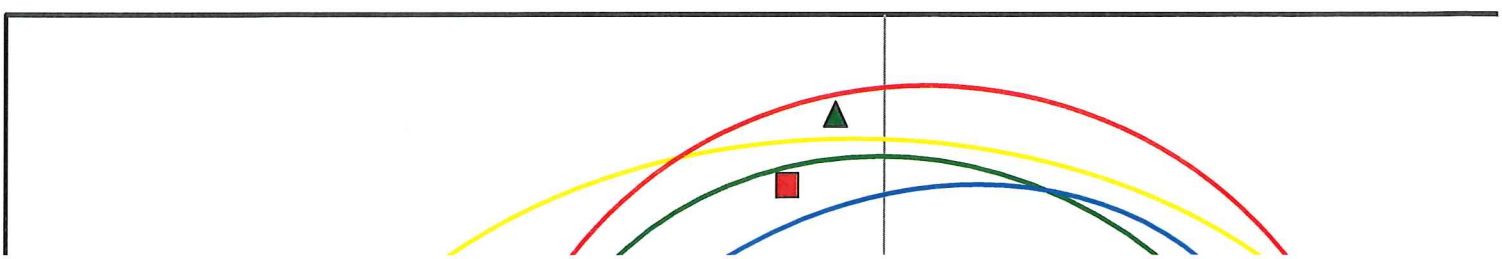

Supplementary Material

The primordial zone (pre-hatching/early larval stage) of the otolith was only faintly visible in most sections (Fig. S1.1). In those sections where the primordium was not clearly visible an estimation of its location was made. Typically the primordium was located on the distal side of the core (which was usually clearly visible) opposite the sulcus indent (Morales-Nin *et al.* 2002; Vieira *et al.* 2009).

Repeated measures Analysis

A 'repeated measures' ANOVA approach (Chambers and Miller 1995) was used to account for non-independence of transect data sampled within each otolith for both microchemical and isotope data and to test whether the mean elemental and isotope ratios differed among sampling locations and between designated life stage data. Residuals of these analyses were tested for normality and homogeneity of variance using Kolmogorov-Smirnov and Levene's tests respectively (Zuur et al. 2007).

Due to values not conforming to the required assumptions of normality and homogeneity of variance, data were $\log_{10}$ transformed after which values were normal but did not have homogeneity of variance (Mn/Ca). Thus, a more conservative alpha level of 0.005 was used to determine significance for all tests (Underwood 1997), which would also lower the possibility of a type I error occurring. Furthermore, Greenhouse-Geisser and Bonferroni corrections were included to adjust the degrees of freedom and the α-level for significance in multiple testing, respectively. Sr/Ca and Mg/Ca were removed from the repeated measures analysis, as their concentrations in otoliths may vary under physiological control (Brown & Severin 2009). In any case, in our study,

26 otolith Mg/Ca and Sr/Ca values were not found to significantly vary among sites ($p < 0.05$). All the above analyses were done using PASW Statistics 18, using the General Linear Model module (full factorial), with life stage as the within-subjects factor (repeated measure) and location as the between subjects-factor.

30

31 ***Isotope depth profiles***

32

33 Measured depth profiles of temperature and salinity for the sample locations were
34 obtained for the year and month of capture of fish from each sample site from
35 oceanographic data collected under the project DEECON (www.imr.no/deecon). Values of
36 δ^{18}Ow (SMOW) were then estimated from known salinities according to the equation
37 $\delta^{18}O_w$ (PDB) = (−21.2 + 0.61S)*0.97002 − 29.9, and profiles of predicted $\delta^{18}O_{oto}$ as a
38 function of depth were produced (Fig. S1.2).

39

40

41 **References**
42

43 Brown, R.J. & Severin, K.P. (2009) Otolith chemistry analyses indicate that water Sr:Ca is
44 the primary factor influencing otolith Sr:Ca for freshwater and diadromous fish
45 but not for marine fish. Can. J. Fish. Aquat.Sci, 66, 1790-1808.
46 Morales-Nin, B., Canha, A., Casas, M., Figuereido, I., Gordo, L.S., Gordon, J.D.M., Gouveia, E.,
47 Pineiro, C.G., Reis, S., Reis, A. & Swan, S.C. (2002) Intercalibration of age readings
48 of deepwater black scabbardfish, *Aphanopus carbo* (Lowe, 1839). ICES J. Mar. Sci.,
49 **59**, 352-364.
50 Underwood, A.J. 1997. Experiments in ecology. Their logical design and interpretation
51 using analysis of variance. Cambridge University Press.
52 Vieira, A., Farias, I., Figueiredo, I., Neves, A., Morales-Nin, B., Sequeira, V., Martins, M. &
53 Gordo, L.S. (2009) Age and growth of black scabbardfish (*Aphanopus carbo* Lowe,
54 1839) in the southern NE Atlantic. Sci. Mar., **73** (S2), 33-46 doi:
55 10.3989/scimar.2009.3973s2033.
56 Zuur, A.F., Ieno, E.N., and Smith, G.M. 2007. Analysing Ecological Data. Springer, New York.

57
58
59

60 **Tables and Figures**
61

62 **Table S1.1**

63

Element	*Location* (F, df, p)	*Life stage* (F, df, p)	*Loc*Life stage* (F, df, p)
Li/Ca	2.67 (3, 82) = 0.053	288.13 (3, 246) < 0.001	1.60 (9) = 0.11
Mn/Ca	1.64 (3, 89) = 0.18	521.7 (2.46, 219) < 0.001	0.93 (7.38) = 0.49
Cu/Ca	0.86 (3, 87) = 0.46	133.5 (3, 261) < 0.001	0.77 (9) = 0.64
Zn/Ca	4.22 (3, 88) = 0.008	81.05 (3, 264) < 0.001	2.80 (9) = 0.004
Ba/Ca	3.34 (3, 89) = 0.02	73.89 (3, 267) < 0.001	3.35 (9) < 0.001

64

65

66 **Table S1.2**

67

Site	Mean Concentration			
	Li/Ca	Mn/Ca	Zn/Ca	Ba/Ca
		Early Larval		
ROC	0.38(0.08)	0.84 (0.17)	4.76 (0.99)	2.19 (0.45)
MAD	0.36(0.08)	0.79 (0.16)	5.35 (1.11)	3.15 (0.65)
AZO	0.37 (0.07)	0.85 (0.17)	2.57 (0.53)	2.09 (0.42)
PTS	0.39 (0.08)	0.84 (0.17)	1.85 (0.37)	2.49 (0.51)
		Late Larval		
ROC	0.37 (0.08)	0.75 (0.16)	3.32 (0.71)	2.26 (0.48)
MAD	0.32 (0.07)	0.67 (0.14)	2.52 (0.52)	2.84 (0.59)
AZO	0.34 (0.07)	0.72 (0.14)	2.07 (0.42)	2.11 (043)
PTS	0.36 (0.07)	0.70 (0.14)	1.40 (0.28)	2.41 (0.49)
		Transition		
ROC	0.32 (0.07)	0.61 (0.13)	2.29 (0.48)	1.59 (0.33)
MAD	0.26 (0.05)	0.50 (0.11)	1.25 (0.26)	2.90 (0.60)
AZO	0.29 (0.06)	0.55 (0.11)	1.68 (0.34)	1.87 (0.38)
PTS	0.31 (0.06)	0.48 (0.09)	0.85 (0.17)	2.48 (0.51)
		Adult		
ROC	0.22 (0.05)	0.27 (0.05)	1.79 (0.37)	1.29 (0.27)
MAD	0.19 (0.04)	0.23 (0.05)	0.74 (0.15)	1.52 (0.31)
AZO	0.18 (0.04)	0.25 (0.05)	1.48 (0.30)	1.54 (0.31)
PTS	0.20 (0.04)	0.24 (0.05)	0.74 (0.15)	1.61 (0.33)

68

69 **Table S1.3.**

70

71

True Group / Classified to:	Rockall				Madeira				Azores				Portugal Slope				Total				%			
	EL	LL	T	A	EL	LL	T	A	EL	LL	T	A	EL	LL	T	A	EL	LL	T	A	EL	LL	T	A
ROC	15	12	9	12	4	3	1	4	2	2	6	4	2	3	4	1	23	20	20	21	65.2	60	45	57.1
MAD	5	6	2	6	10	10	15	8	2	0	0	1	5	4	4	6	22	20	21	21	45.2	50	71.4	38.1
AZO	7	6	7	5	2	6	7	6	4	2	6	5	10	10	4	8	23	24	24	24	17.4	8.3	25	20.8
PTS	2	5	6	3	5	3	7	5	8	3	4	2	9	11	5	12	24	22	22	22	37.5	50	22.7	54.5

Table S1.4

Location	*T(°C) at capture*	*Salinity at capture*	*Season Of Capture*	*J $\delta^{18}O$ (‰)*	*J $\delta^{13}C$ (‰)*	*ML $\delta^{18}O$ (‰)*	*ML $\delta^{13}C$ (‰)*	*A $\delta^{18}O$ (‰)*	A $\delta^{13}C$ (‰)
PTS	11.4	36.2	Autumn	1.18	-5.71	1.50	-4.65	2.17	**-2.54**
MAD	8.9	35.7	Winter	1.34	-5.04	1.86	-3.93	2.34	**-2.05**
ROC	10.1	35.6	Autumn	0.91	-6.09	1.63	-4.71	2.19	**-3.11**
AZO	5.7	35.2	Summer	1.05	-5.69	1.35	-5.11	2.66	**-2.04**
Overall Mean	9.02	35.7	-	1.21	-5.44	1.56	-4.64	2.32	**-2.40**

78

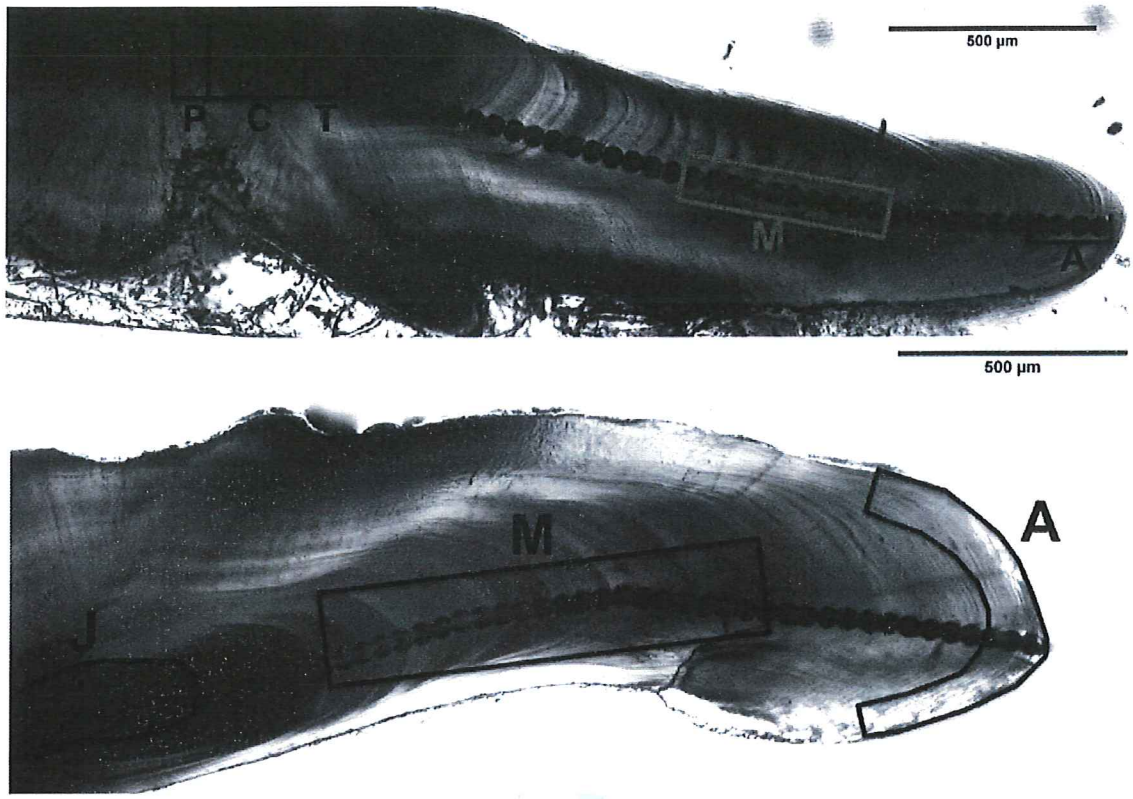

79

80

81 **Fig. S1.1**

82

83

84

85

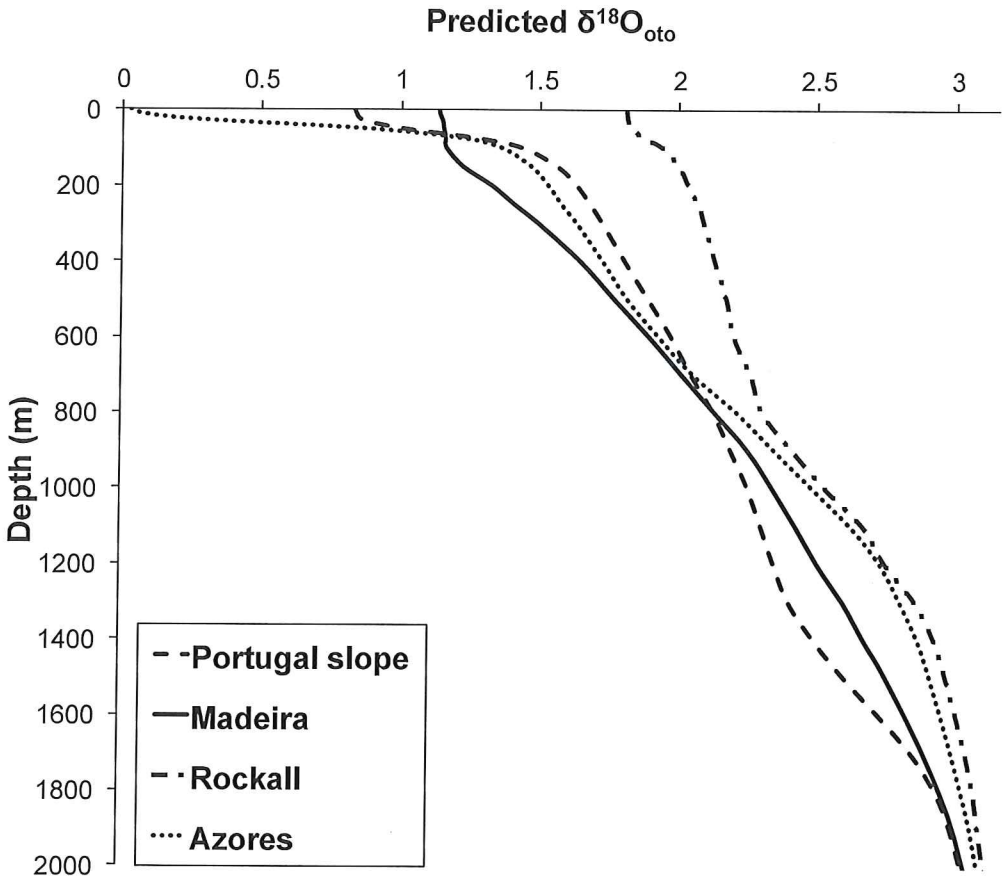

86

87

88 **Fig. S1.2**

89

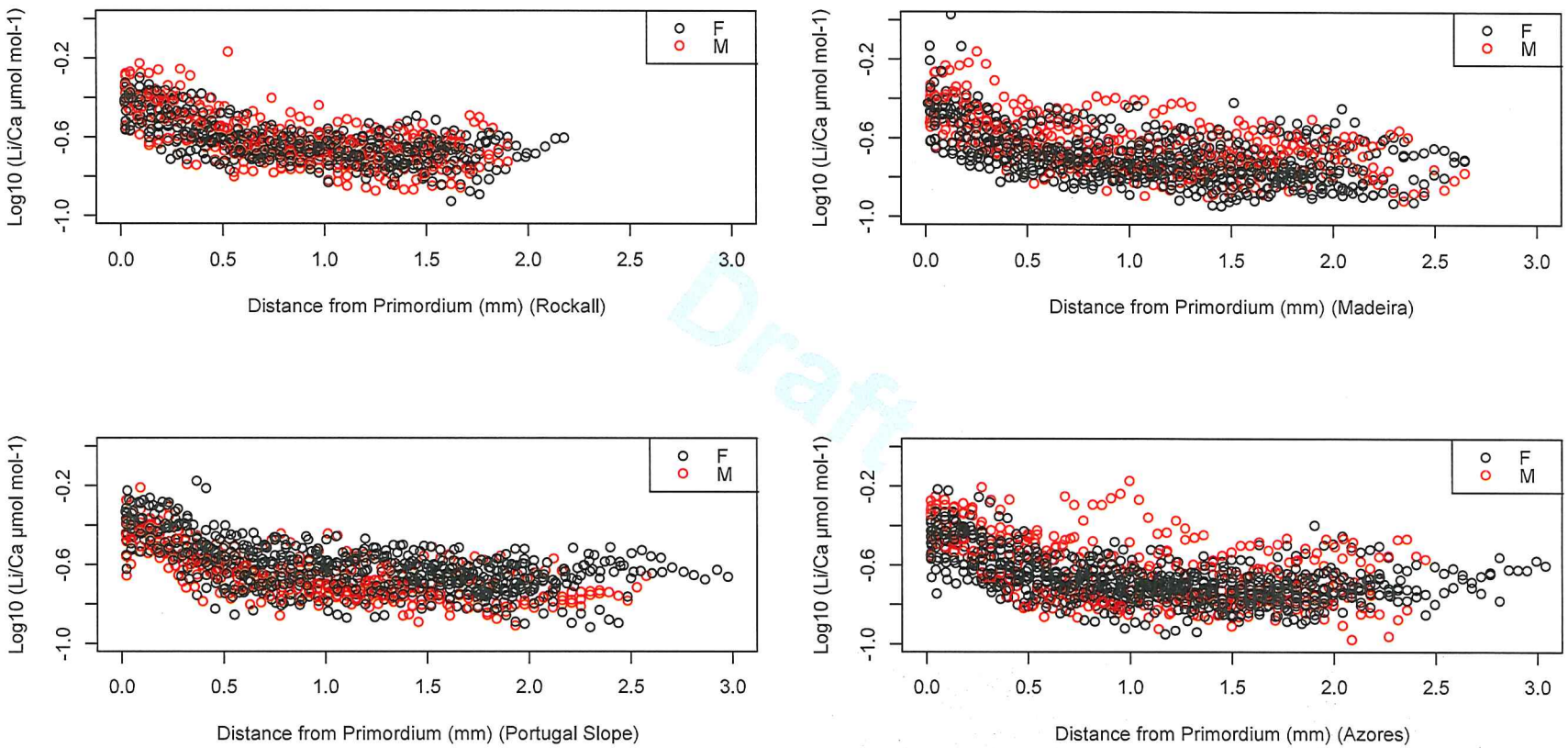

Fig. S1.3

94

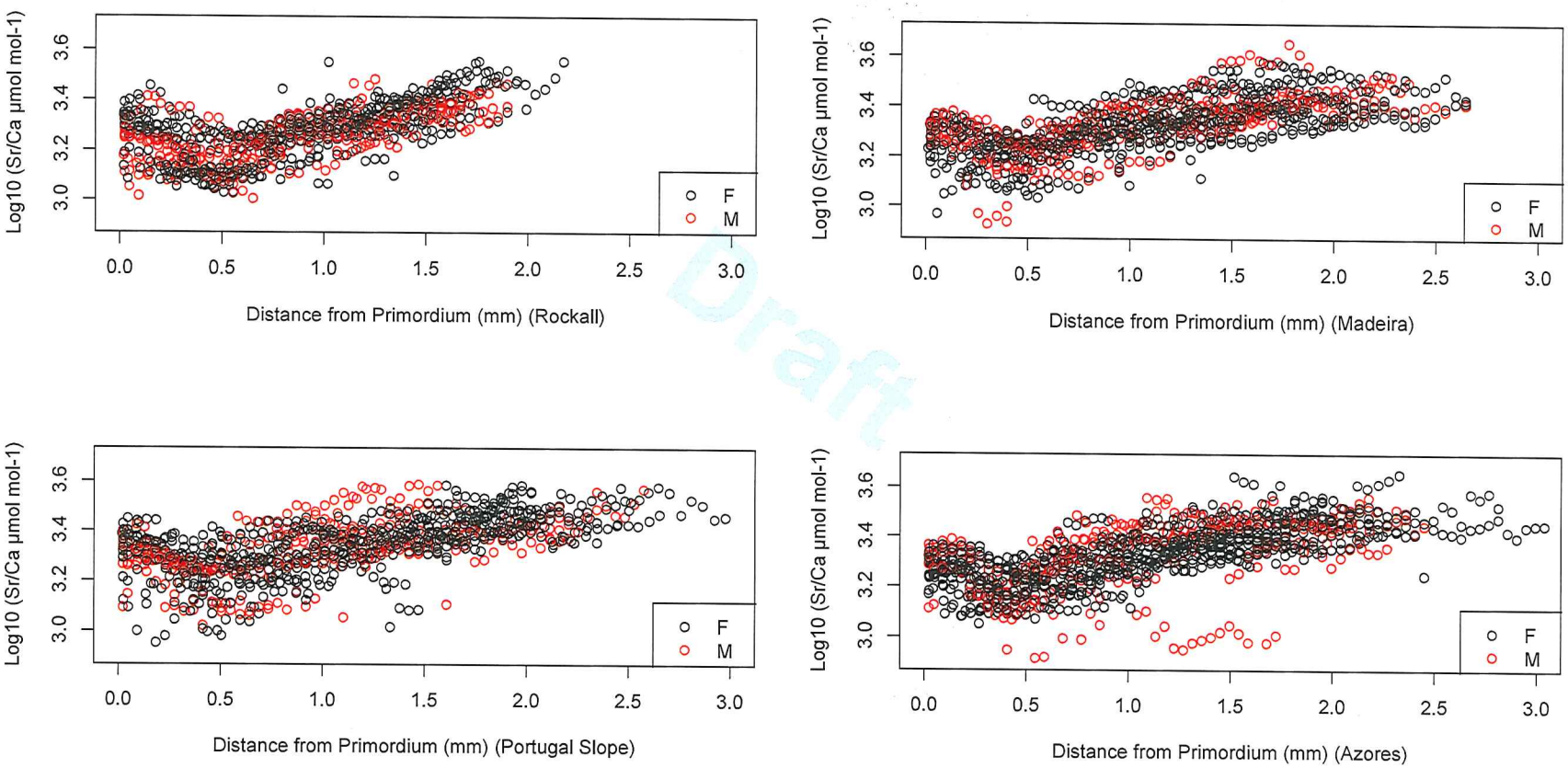

95
96 **Fig. S1.4**

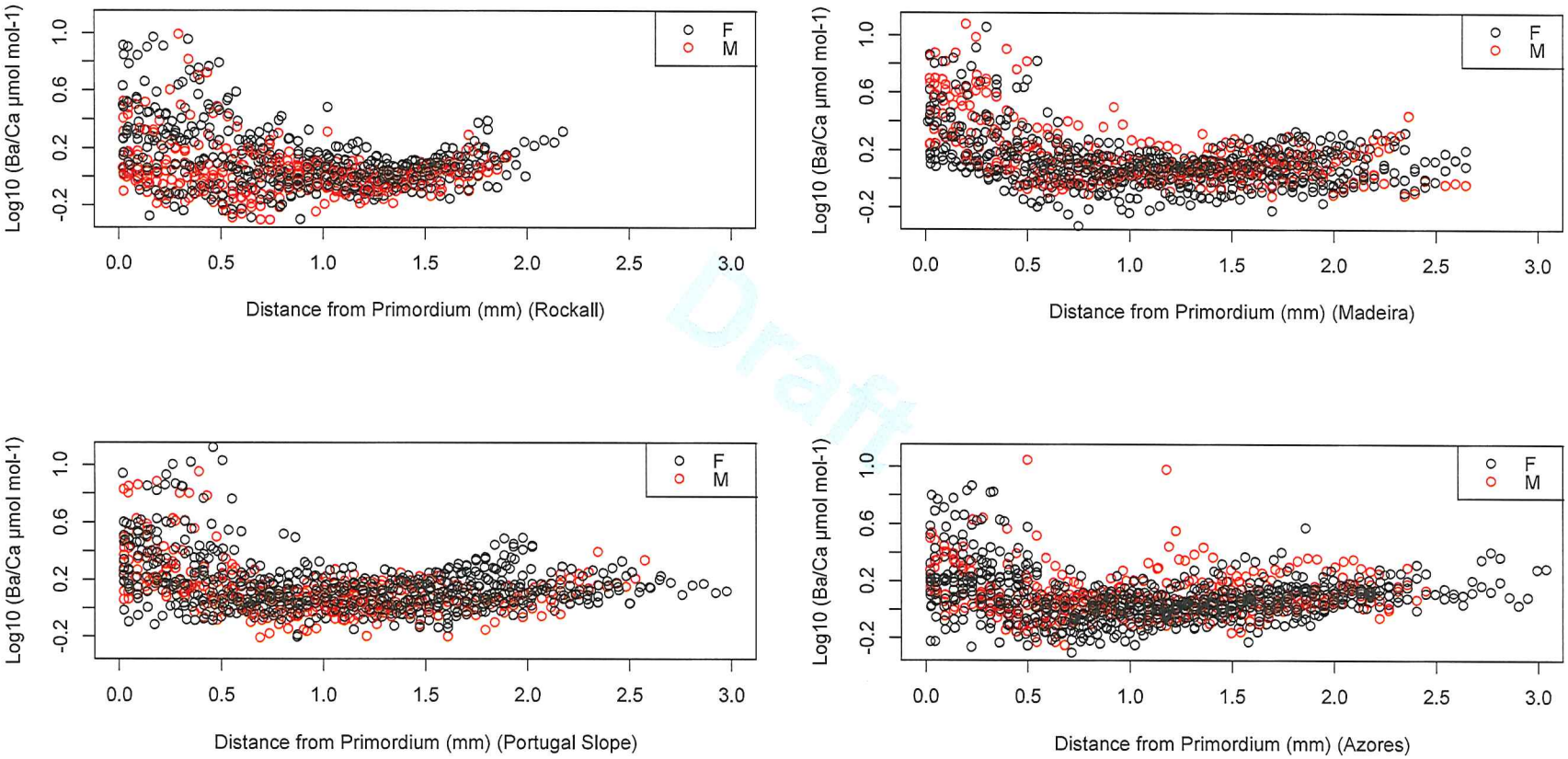

Fig.S1.5

100

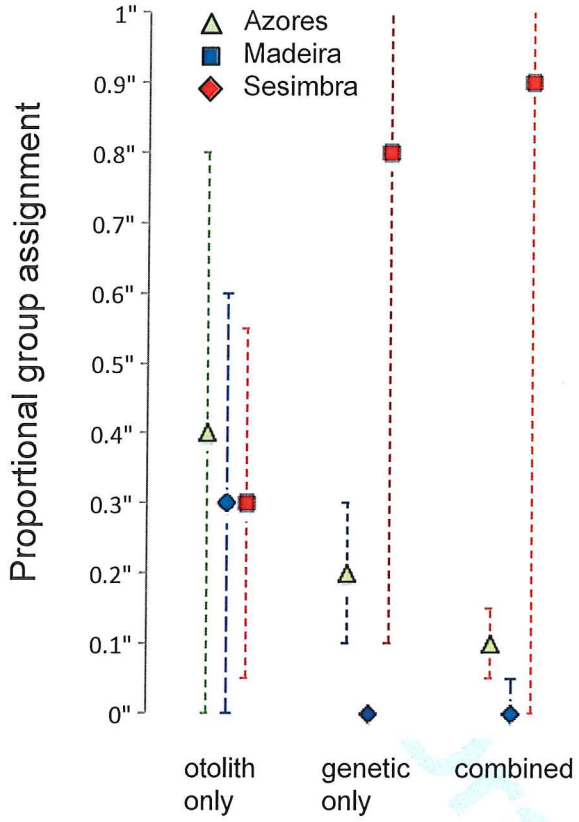

101

102 **Fig. S1.6**